Parameter estimation of an experimental rotor dynamic set-up

Eindhoven University of Technology, department of Mechanical Engineering

Parameter estimation of an experimental rotor dynamic set-up

T.A.M. Wegman

DCT no. 2006.22

Bachelor Thesis
Dynamics and Control group

Supervisors:
Prof. dr. H. Nijmeijer
Dr. ir. N. van de Wouw

Coaches:
Ir. A. Doris
Ing J.C.A. de Bruin

Eindhoven, February 2006

Summary

In this thesis an experimental set-up, which represents a rotor dynamic system with dry friction, is considered. Such a system can be used to describe some dynamical phenomena which occur in a real drill string set-up, as used by oil companies. These drill strings mainly consist of a rotating load (drilling bit), which is driven by a power source and a low stiffness string. In the experimental set-up, as in a real drill string set-up, the rotating load stalls repetitively for a range of input signals. Such a stick-slip motion is undesirable since it limits the drilling efficiency and service life of the drilling bit. In order to predict the rotational motions of the experimental set-up, a dynamic model of the set-up is formulated. The parameters of the dynamic model are unknown and need to be identified.

The dynamical behavior of the experimental set-up is similar to a real drill string system. However, in real drill string systems there are also lateral vibrations, while these are suppressed in the experimental set-up. This is done since attention goes to rotational dynamics only.

The experimental set-up mainly consists of an upper disc and a lower disc, which are connected to each other by a low stiffness string. The upper disc is driven by a DC motor, which is regulated by a predefined input voltage. The movement of the lower disc depends on the motions of the upper part since they are attached to each other by the string. Due to the low stiffness of the string and friction present at the lower disc, the movement of the lower disc differs from that of the upper disc. The effect that the input voltage has on the movement of the upper and lower disc, is described by stating the equations of motions of the set-up. In this work, the parameters at the equations of motion are estimated in an iterative way, by using a nonlinear least squares method. The better the quality of the estimated parameter set, the more accurately reality is described by the dynamic model.

The error between measured data and simulated data is very small in most cases. However, such prediction errors will always occur. The reason for that is that a model can not describe reality perfectly. Also, there is unavoidable noise in the measurements.

Table of contents

Chapter 1

Introduction

In this thesis an experimental set-up, which represents a rotor-dynamic system with dry friction, is being considered. Such a system can be used to describe some phenomena which occur in real drilling systems. The drill pipe in such a drilling system can be as long as 3 to 8 km. Because of the length of the pipes and the varying forces acting on the drilling bit, the speed of the drilling bit varies and the string winds up. Problems arise when due to high friction forces the bit stalls. In that situation the string winds up further and builds up torque until the bit rotates again. This process of winding and unwinding is a kind of vibration phenomenon (stick-slip vibrations), which lowers drilling efficiency and the maximum service life of the drilling-bit.

The experimental set-up has been designed and constructed in the laboratory of the Dynamics and Control group. It is not an actual model of a drilling system, but its dynamical behavior is very similar in the sense that stick slip vibrations also occur while their cause can be investigated more closely. The parameters which regulate the motions of the experimental set-up are to be estimated. Previous modeling and estimation results for the set-up can be found in [2] and [4]. However, since the experimental set-up has been adapted partially, its parameters are estimated again in this thesis.

This thesis is organized as follows: in chapter 2, the set-up is described in detail, in order to provide good understanding about the way it functions and which processes regulate its motions. Moreover, the model of the set-up is introduced. In chapter 3, the complete parameter estimation procedure is described. The accuracy and reliability of the parameter estimation procedure with regard to the experimental set-up is examined in chapter 4 using simulated data. In chapter 5, the actual parameter estimation is carried out for the experimental set-up. Finally, conclusions on the parameter estimation results of the experimental set-up are given in chapter 6.

Chapter 2

The set-up

In this chapter, the experimental set-up is described. The set-up (figure 2.1) mainly consists of a DC motor and two discs which are connected by a low stiffness string (mechanical part of the set-up). Also, a set of hardware and software devices is used for measuring specific system parameters (measuring equipment).

The mechanical model is mounted between two vertical beams. It consists of the upper part and lower part, which are connected with a low stiffness string. At the left of figure 2.1 and in figure 2.2, the measurement equipment is visible.

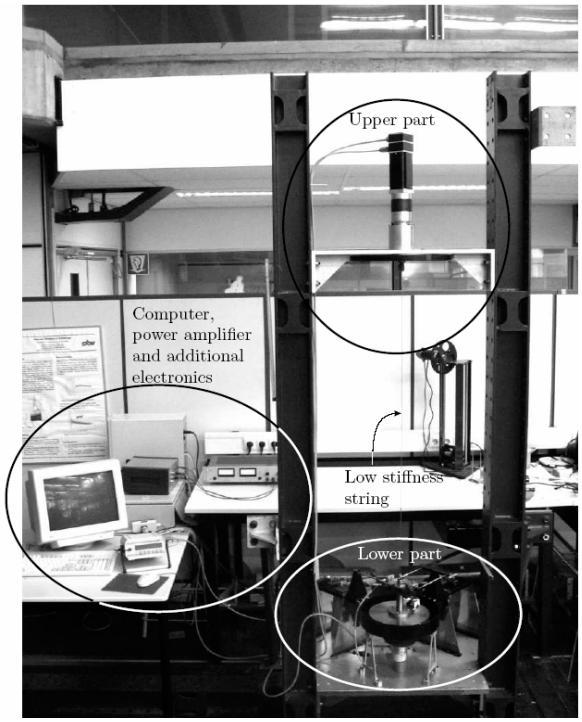

Figure 2.1: Total set-up [2].

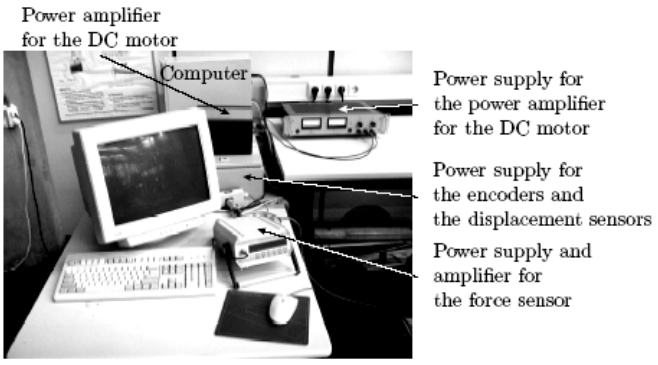

Figure 2.2: Computer, power amplifier and power supplies of the set-up [2].

2.1 Mechanical part

The upper part of the set-up (figure 2.3) consists of a steel disc, a DC motor and an encoder. The DC motor drives the upper disc via a gear reduction (ratio 3969/289). The encoder is attached on top of the motor to measure the rotation of the axis of the DC motor, from which the rotation of the upper disc is derived. On the bottom of the upper disc a low stiffness steel string is attached, which connects the upper and lower disc.

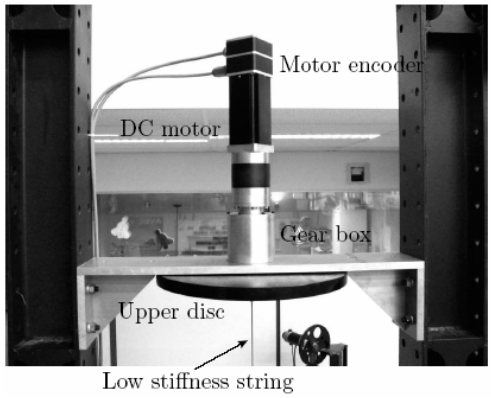

Figure 2.3: The upper part of the set-up [2].

The lower part of the set-up (figure 2.4) consists of a brass disc which is connected to the upper disc by the low stiffness steel string. The encoder of the lower part is mounted on the lower bearing housing. This encoder measures the angular displacement of the lower disc.

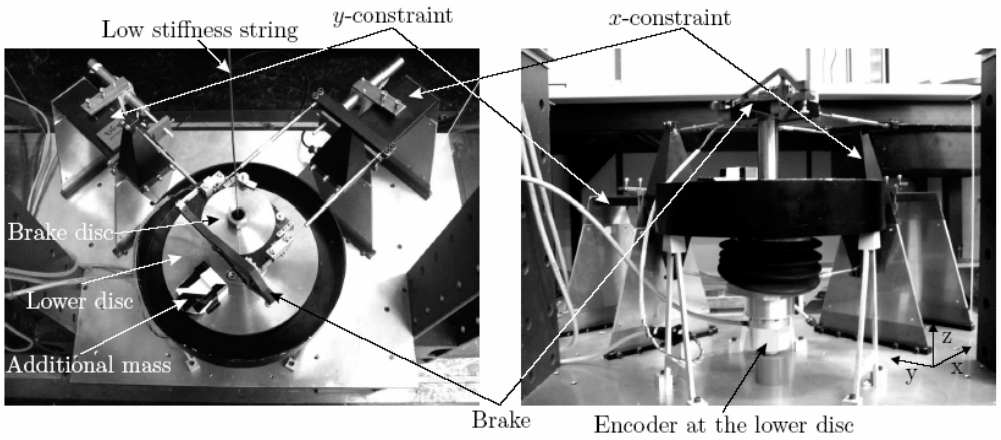

Figure 2.4: The lower part of the set-up [2].

On the top of the lower disc, a brake disc is mounted by means of a very stiff shaft (see figure 2.5). Two bronze brake blocks apply a normal force on the brake disc. The magnitude of the normal force can be adjusted with a screw. In this way, a range of normal forces can be chosen, such that the friction acting on the lower disc can be adjusted.

For real drilling systems it has been observed that stick slip vibrations occur between the drilling bit and borehole when a region of negative damping is present in the friction curve [4]. Earlier investigations on the experimental set-up investigated here, have shown that lubrication between the brake disc and brake blocks is essential for the occurrence of negative damping. Therefore, a little oil box is attached on top of the upper bearing housing of the lower disc (figure 2.5). Using the capillary properties of felt, a constant flow of oil to the brake disc is ensured. Ondina oil has shown to have favorable properties for creating negative damping [4].

Furthermore, a force sensor is attached to the brake by a rod (figure 2.5). By measuring the distance of the brake blocks to the geometric center of the brake, the friction torque exerted on the lower disc can be calculated from such force measurements.

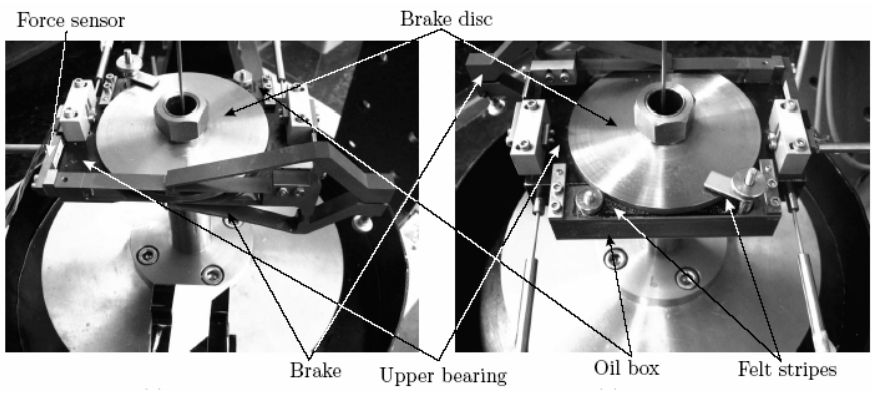

Figure 2.5: Brake and oil box with felt stripes [2].

Both the upper and lower disc can only rotate around their geometric centers (there are no other degrees of freedom). However, by removing the constraints in x- and y-direction it is possible to let the lower disc move in the lateral plane. For this purpose, an extra mass was added on top of the lower disc (see figure 2.4) to induce movements in the lateral plane. The constraints in x- and y- direction are depicted in figures 2.6 and 2.7. Each constraint consists of a parallel leaf spring in x or y-direction, which are connected by three or two rods respectively to the lower and upper bearing housing of the lower part. These constraints also prevent the disc from tilting.

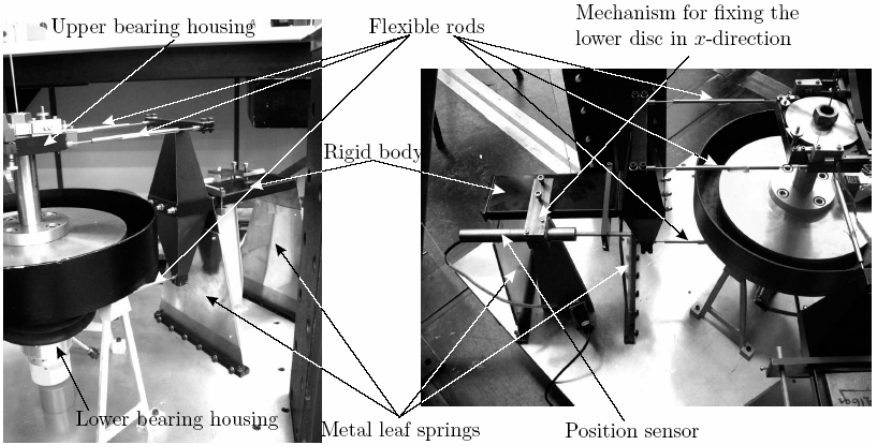

Figure 2.6: A front and a rear view of the x-constraint [2].

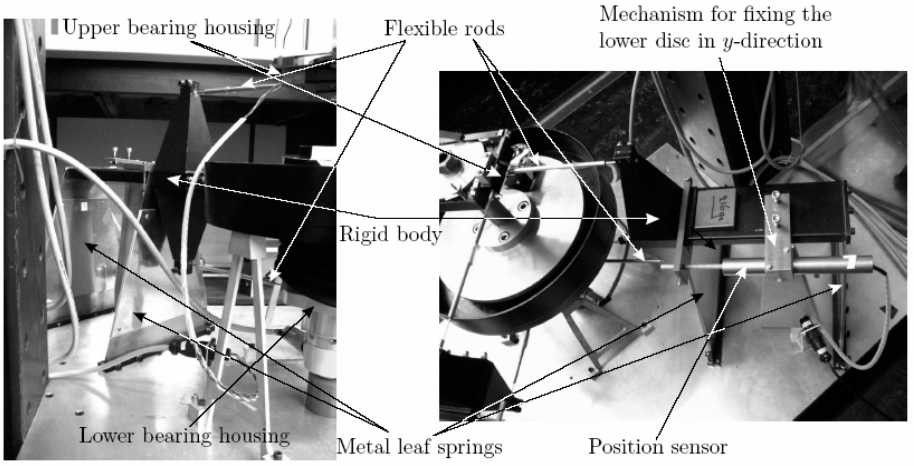

Figure 2.7: A front and a rear view of the y-constraint [2].

Since this thesis is focused on the rotational dynamics of the experimental set-up only, the x- and y-constraints will always be fixed; so there are no movements in the lateral plane. The extra mass is not removed in order to keep the set-up in the same state as it was when the earlier measurements were done.

2.2 Measuring equipment

The measurement equipment consists of a computer, a DAC (Digital to Analogue Converter) and an amplifier. The computer is used to generate the input signal and to retrieve experimental data. The software program used for this purpose is Simulink. Using Simulink, the DAC and the amplifier, a voltage which is limited to the range of -5V +5V is fed into the DC motor, at the upper part of the set-up. Subsequently the upper disc is driven via the gear reduction.

The angular positions of the upper and lower disc are measured using incremental encoders. The encoder at the lower part of the set-up measures the angular displacement of the lower disc (there are 10000 counts per revolution). With the aid of a quadrature decoder, the number of counts is increased by factor 4, resulting in a resolution of 40000 counts per revolution. The encoder of the upper part measures the revolutions of the motor axis instead of the revolutions of the upper disc itself. Moreover, this encoder only has 1000 counts per revolution. Since there is a gear reduction and by again using the quadrature decoder, we attain a resolution of 1000*4*3969/289= 54934,256 counts per revolution of the upper disc. The angular velocities of the upper and lower disc are calculated by numerically differentiating the respective angular positions with respect to time.

2.3 Model of the set-up

In this section, the model of the experimental set-up is presented. Several assumptions are made for that purpose, to ensure that the dynamic model of the experimental set-up is accurate without unnecessarily taking complex phenomena into account. The assumptions are:

- Since the string does not wind over many rotations, it is assumed that the lower disc does not move in vertical direction;
- The lower disc always remains horizontal;
- Torsional damping in the string is very small compared to the damping at the upper and lower part, and therefore it is not modeled.

Schematically, the set-up can be depicted as in figure 2.8. The figure represents a computer and a power amplifier applying an input voltage u to the DC motor at the upper part of the set-up. This causes the radial position of the upper disc to change. Since the lower disc is attached to the upper disc by the low stiffness string, the lower disc starts to rotate as well. The dynamics of the total set-up are described by two differential equations, which are derived using Euler's axiom:

$$J_u\ddot{\theta}_u + T_{fu}(\dot{\theta}_u) - k_\alpha\alpha = k_m u\,, \tag{2.1}$$

$$J_l\ddot{\theta}_l + T_{fl}(\dot{\theta}_l) + k_\alpha\alpha = 0\,, \tag{2.2}$$

with

$$\alpha = \theta_l - \theta_u\,. \tag{2.3}$$

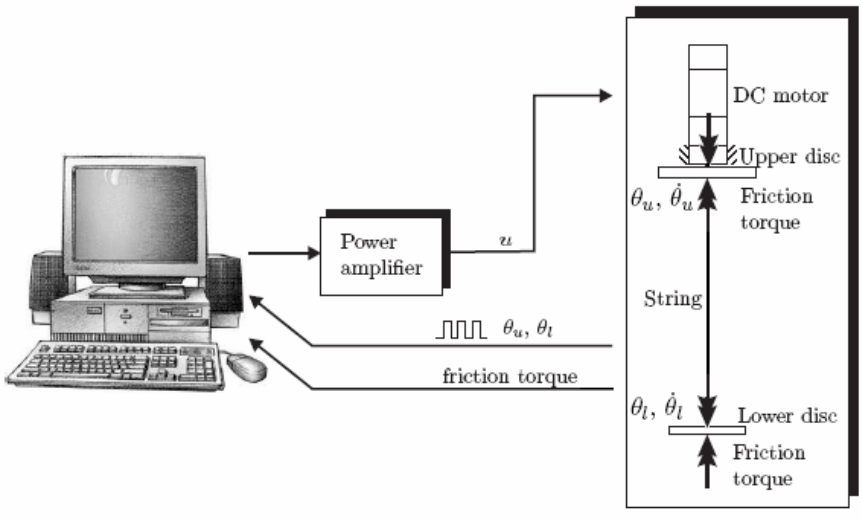

Figure 2.8: Schematic representation of the set-up [4].

The subscripts u and l have been used to make a distinction between parameters representing the upper and lower part of the set-up. T_{fu} and T_{fl} represent the friction torque at the upper and lower disc respectively, and J_u and J_l are the moments of inertia of the upper and lower discs about their respective centers of mass. The stiffness of the string is represented by k_α and the motor constant by k_m. The angular displacement, velocity and acceleration of both discs are represented by θ_u, $\dot{\theta}_u$ and $\ddot{\theta}_u$, and θ_l, $\dot{\theta}_l$ and $\ddot{\theta}_l$ respectively. Equations (2.1) and (2.2) describe the angular dynamics of the upper and lower part respectively. The difference between the angular positions of the lower and upper disc is represented by the angle α ((2.3)).

The friction torque functions T_{fu} and T_{fl} for the upper and lower part are pretty similar when the brake is not applied. These functions then are represented by a combined Coulomb and viscous friction function; the form of such a friction model is given in (2.4) and (2.5). However, the upper and lower part do not have the same Coulomb and viscous friction parameters Tc and b.

$$T_{fd}(\dot{\theta}) = \begin{cases} T_d(\dot{\theta})sign(\dot{\theta}) & for \quad \dot{\theta} \neq 0 \\ [-T_d(0), T_d(0)] & for \quad \dot{\theta} = 0, \end{cases} \qquad d = \{u, l\} \tag{2.4}$$

with

$$T_d(\dot{\theta}) = Tc_d + b_d\left|\dot{\theta}\right|. \tag{2.5}$$

If the brake is applied to the lower part of the experimental set-up, (2.5) changes into (2.6). This is because the negative damping contribution of the brake needs to be taken into account. Clearly, (2.6) only applies to the lower part of the set-up.

$$T_l(\dot{\theta}_l) = Tc_{lb} + b_{lb}\left|\dot{\theta}_l\right| + (Ts_{lb} - Tc_{lb})e^{-\left(\frac{|\dot{\theta}_l|}{\omega_{slb}}\right)^{\delta_{slb}}}, \tag{2.6}$$

where Ts_{lb} represents the static friction level, Tc_{lb} the Coulomb friction level, ω_{slb} the Stribeck velocity and δ_{slb} is the Stribeck shape parameter. In the next chapters, the parameters stated in the equations of motion are joined in a parameter set P, to improve readability.

The friction function T_{fd}, as stated in (2.4), is non-linear in the sense that there is a step in the friction torque when angular velocity changes sign. To model this discontinuity, conditions are imposed on the dynamic model, using the switch model [4],[5]. When the absolute velocity is smaller than a very small value (10^{-6} rad/s), a different equation of motion is prescribed. This way the need of very small computational steps when velocity approaches 0 rad/s is avoided. This means that the differential equation does not need to make very expensive calculations (high calculation time) around 0 rad/s.

Chapter 3

Parameter estimation method

In the previous chapter, the dynamic model for the experimental set-up has been formulated. In this model of the set-up (see (2.1)-(2.6)), all parameters are unknown and need to be identified. In this chapter, the method for the estimation of the parameters of the equations of motion of the set-up is presented. The estimation method consists of a minimization algorithm and a suitable input signal for the DC motor. A measure for the quality of the estimated parameters is proposed in the form of the R^2-criterion which is used in validating the estimated parameters. For validation purposes, a different input signal is used.

3.1 Estimation procedure

The minimization algorithm is such that previously estimated parameter values for the dynamic model of the experimental set-up, are adapted and applied again to the dynamic model. The objective of the algorithm is to minimize the error between experimental and simulated data. Simulated data are obtained by applying the estimated parameter values and an input signal to the model. To minimize the error between experiment and simulation, a (non-linear) least squares procedure is chosen. Herein, the following objective function is being minimized

$$\min \sum_{i=1}^{n} \left(y_i - \hat{y}_i(P_j) \right)^2 \tag{3.1}$$

In (3.1), y_i represents an element of the experimental data set y and $\hat{y}_i$ an element of the simulated data set $\hat{y}$. These data sets consist of n elements. The simulated data is produced by applying parameter set P_j and input signal u to the model of the set-up. P_j represents the set of estimated parameter values which is calculated after iteration step j. The minimization procedure is stopped when the objective function is smaller than a predefined tolerance, or if the difference between the values of the previous and the current set of parameters is smaller than a predefined tolerance. The execution of (3.1) is performed in Matlab with the 'lsqnonlin' command. This command repetitively calls upon the m-files in which the dynamic model of the set-up is stated. Before the estimation procedure can be started, a set of initial parameters P_0 has to be provided to the model. If after j iterations one of the predefined tolerances is met, the final set of parameters P is given (which equals P_j). This is summarized in the scheme as depicted in figure 3.1.

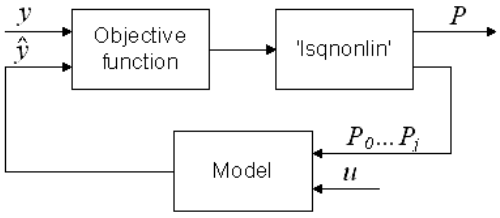

Figure 3.1: Scheme of the minimization procedure.

If an initial parameter value is not close enough to the real parameter value, the least squares procedure possibly converges to a local minimum. This implies that iteration stops, since one of the previously defined stopping criteria is met, while the finally estimated set of parameters P does not describe reality well.

The correctness of the estimation thus needs to be checked. This is done by studying the error between experiment and simulation and validating the quality of the estimated parameters. Moreover, an objective measure for the quality of the estimation is used, which is stated in section 3.3.

3.2 Input signals

To estimate all parameters which are needed to accurately describe the dynamics of the experimental set-up (see section 2.3), all relevant dynamics in the set-up need to be excited. Otherwise, it is possible that some dynamical phenomena and the accompanying parameters that are to be estimated, do not come to light in the experiment while they possibly do in other situations. To avoid the latter scenario, a proper input signal has to be applied to the DC motor. Since relevant dynamics are below 5 Hz and to avoid damage to the set-up, the following input voltages for the DC motor are used (figure 3.2):

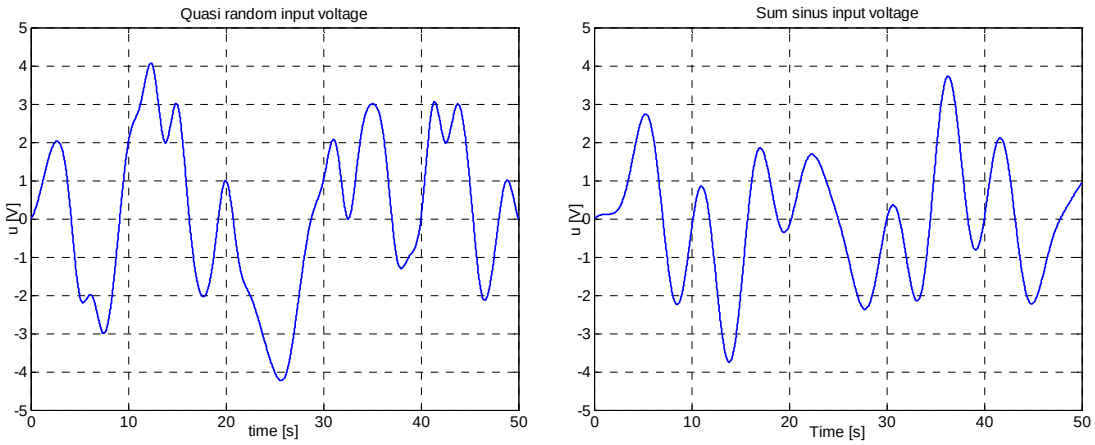

(a) Estimation input voltage u_{est}.

(b) Validation input voltage u_{val}.

Figure 3.2: Input signals $u_{est}(t)$ and $u_{val}(t)$ used for estimation and validation, respectively.

These signals do not contain frequencies above 5 Hz and the voltage is limited between -5V and +5V. The quasi random input voltage u_{est} is used to estimate the parameters. The second signal, the validation input voltage u_{val}, is a sum of various sinus functions. It is used to validate the parameter set which is determined using the response of the experimental set-up to the estimation input signal. If the validation results are good as well, it is plausible that the estimated parameter set is correct for other input voltages too. In [2] and [4], these signals were used as well.

3.3 R^2-criterion

In order to have an objective measure about how accurately the simulated data resembles experimental data, the R^2-criterion is used

$$R^2 = 1 - \frac{\sum_{i=1}^{n} \left(y_i - \hat{y}_i(P_i)\right)^2}{\sum_{i=1}^{n} \left(y_i - \bar{y}\right)^2}, \tag{3.2}$$

where $\bar{y}$ represents the mean value of the experimental data, y_i an element of the experimental data set and $\hat{y}_i$ an element of the simulated data set. From (3.2) it is clear that the maximum value of R^2 equals 1. Values close to 1 indicate a very high resemblance of the simulated data compared to the experimental data, thus indicating a high quality of the estimated parameter set.

3.4 Overview of the parameter estimation method

In the next chapters, the parameters of the upper part and lower part of the set-up and the brake are estimated. The following steps are taken. First the dynamic model of the considered part is formulated. Then an earlier estimated parameter set P_{ref} from [2] is used and the estimation signal u_{est} is applied to the dynamic model of the set-up. This yields a data set y_{ref} which resembles the experimental angular displacement data, because the parameter estimation in [2] was shown to be very accurate. This implies that the real set-up is described with high accuracy. However, this data set is generated by the dynamic model, so it is a simulated data set. Analogously a data set y_{val} is created. These procedures are shown in figure 3.3.

(a) Simulated estimation results y_{ref}. (b) Simulated validation results y_{val}.

Figure 3.3: Simulated data set generation.

Subsequently, this simulated data set is used as the reference input y_{ref} for the parameter estimation procedure. That is: the simulated data set y_{ref} is treated as a real experimental set from which the parameters are to be estimated. To start the estimation procedure, an initial set of parameters P_0 and the estimation voltage u_{est} have to be provided to the model. In order to acquire understanding about the influence of the initial set of parameters on the estimation results and about the accuracy of the minimization procedure, P_0 differs slightly from P_{ref}. Furthermore, the influence that the difference between P_{ref} and P has on the error between experiment and simulation, can be investigated closely.

The iterative process of parameter estimation continues until after j iterations the predefined tolerances in Matlab command 'lsqnonlin' are satisfied, yielding parameter set P. Subsequently, the set P and the input signals u_{est} and u_{val} from figure 3.2 are applied to the model yielding simulated sets $\hat{y}_{est}$ and $\hat{y}_{val}$, for the estimation and validation signal respectively. Note that these simulated sets are calculated using P instead of P_0.

Finally, the R^2-criterion regarding the estimation and validation results gives a measure for the correctness of the estimated parameter set. If the R^2-value is too low, P_0 is adapted and the procedure is started again. This procedure is shown schematically in figure 3.4. The left part of the scheme represents the estimation procedure, while at the right part the parameter estimation result P (which equals P_j) is processed.

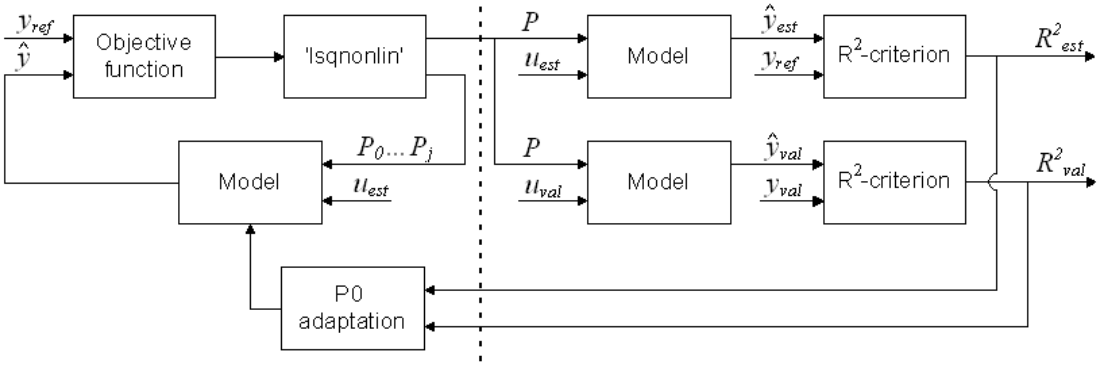

Figure 3.4: Scheme of the complete parameter estimation procedure.

Next, the parameters of the real experimental set-up are determined. The procedure is almost the same as was described in the foregoing and as shown in figure 3.3. However, instead of simulating the sets y_{ref} and y_{val}, these are obtained by applying the estimation and validation input voltages from figure 3.2 to the DC motor. Then, the angular displacements θ_u and θ_l of the upper and lower disc are measured for the two input voltages and result in two sets; y_{ref} and y_{val}. The experimental results which are used here, are taken from [2] and [4].

To keep the complexity of the estimation procedure as low as possible, the parameters of the experimental set-up are determined in three steps. However, the estimation procedure for these three steps is the same: first, a model of the respective part is formulated, and then the parameters of the model are estimated.

The parameters of the upper part are determined first. Next, the parameters in the equation of motion for the lower part, without applying the brake, are determined. Finally, the parameters which describe the friction of the brake are determined. In chapter 4, the parameter estimation procedure is carried out on simulated data sets, which are obtained as is described in this section. In this way, the accuracy of the estimation procedure and the influence of the initial set of parameters P_0 can be studied. In chapter 5, the parameters of the equations of motion of the experimental set-up are determined using actual measurements.

Chapter 4

Parameter estimation using simulation results

Before the parameters of the set-up are estimated from a real experiment, the estimation procedure is executed on simulated measurement data of the set-up. In this way, the influence of the initial set of parameters P_0 and the accuracy of the parameter estimation method can be investigated closely. Simulated measurement data are obtained by applying the estimated parameter set P_{ref} from [2] to the dynamic model, as was described in section 3.4.

4.1 Upper part of the set-up

4.1.1 Modeling the upper part

In order to ensure that the lower part does not influence the dynamical behavior of the upper disc, the string is removed. The equation of motion for the upper part is given by

$$J_u\ddot{\theta}_u + T_{fu}(\dot{\theta}_u) = k_m u \,, \tag{4.1}$$

where J_u is the moment of inertia of the upper disc about its center of mass, T_{fu} the friction function and k_m a motor constant. When a sinusoidal signal is applied to the DC motor, it is observed that the displacement of the upper disc is larger for positive angular velocities than it is for negative velocities. This implies the friction torque for positive velocities is lower than it is for negative velocities, so an asymmetric, combined Coulomb viscous friction model is used:

$$T_{fu}(\dot{\theta}_u) = \begin{cases} T_u(\dot{\theta}_u) sign(\dot{\theta}_u) & for \quad \dot{\theta}_u \neq 0 \\ [-T_u(0), T_u(0)] & for \quad \dot{\theta}_u = 0 \end{cases} \tag{4.2}$$

with

$$T_u(\dot{\theta}_u) = Tc_u + \Delta Tc_u sign(\dot{\theta}_u) + b_u\left|\dot{\theta}_u\right| + \Delta b_u \dot{\theta}_u \,. \tag{4.3}$$

Tc_u represents the Coulomb friction and b_u the viscous friction contribution to the friction model.

4.1.2 Parameter estimation using a simulated measurement

As was described in chapter 3, the set of parameters P_{ref} as found in [2] and the estimation signal (see figure 3.2a) are applied to the dynamic model which is stated above. This results in a simulated angular displacement θ_u as shown in figure 4.1. Next, the parameters of the model that describes the displacement of the upper disc are determined by minimizing the following function:

$$\min \sum_{i=1}^{n} \left(\theta_{u,i} - \hat{\theta}_{u,i}\right)^2 . \tag{4.4}$$

To start the parameter estimation procedure, an initial set of parameters P_0 has to be given (see table 4.1). The parameter set resulting from the minimization procedure is denoted by P (table 4.1). It is clearly visible that P differs from $P_{ref.}$, which is caused by the rather big initial difference between P_0 and $P_{ref.}$ It is visible that P is closer to P_{ref} than it is to P_0. This indicates that in this case the minimization procedure converges to P_{ref}. For smaller initial differences between P_{ref} and P_0, P resembles P_{ref} very well. However, studying the influence that a big initial difference has on the finally estimated parameter set, gives a better understanding about the nature of the minimization procedure. Applying P to the model results in an angular displacement $\hat{\theta}_u$ as depicted in figure 4.1 and an error $\theta_u - \hat{\theta}_u$. The R^2-criterion equals 1.0000 for the estimation and 0.9998 for the validation results, which indicates very high resemblance between the estimated and simulated displacement.

Table 4.1: Estimated parameterset P, describing the simulated displacement.

	k_m [Nm/V]	Tc_u [Nm]	ΔTc_u [Nm]	b_u [Nms]	Δb_u [Nms]
P_{ref}	4.3228	0.3798	-0.0058	2.4245	-0.0084
P_0	6.0000	1.0000	0.0000	4.0000	-0.2000
P	4.5743	0.4757	-0.0046	2.5523	0.0022

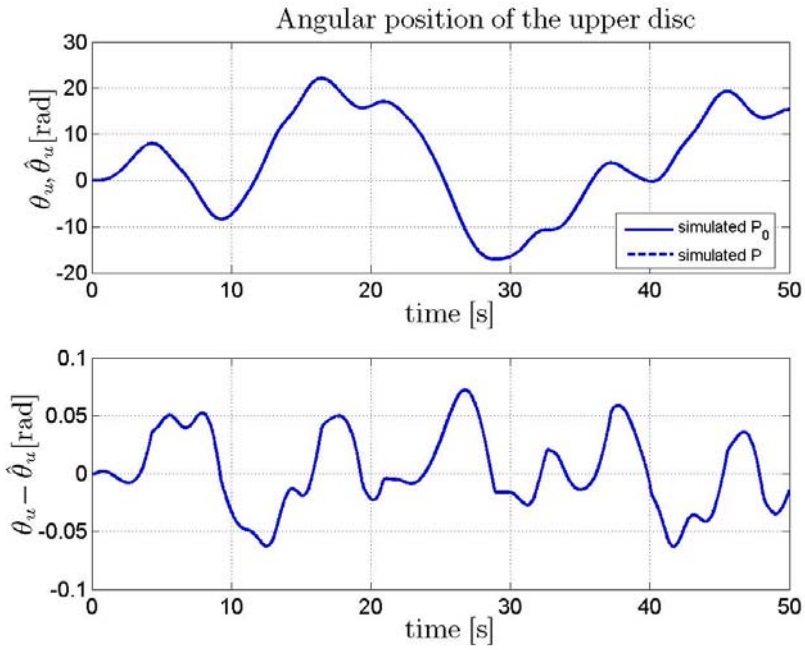

Figure 4.1: Estimation results for θ_u, using a simulated data set; R^2=1.0000.

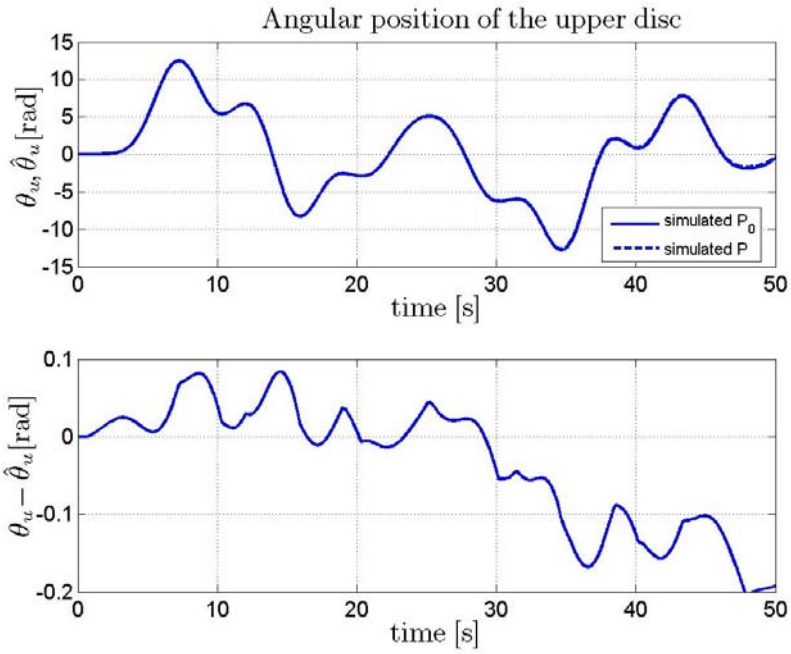

Figure 4.2: Validation results for θ_u, using a simulated data set; R^2=0.9998.

4.2 Lower part of the set-up

4.2.1 Modeling the lower part

In this section, the estimation procedure is carried out using the simulated displacement of the lower part of the set-up. The lower part of the set-up is driven by the upper part, so the string is attached to the upper and lower disc. The brake is not applied. In this case, there are two equations of motion needed to model the dynamic behavior of the set-up, since the total system consists of the upper part which drives the lower part. This causes the equation of motion for the upper part (4.5) to differ from (4.1), because the string is attached:

$$J_u\ddot{\theta}_u + T_{fu}(\dot{\theta}_{u)} - k_\alpha\alpha = k_m u\,, \tag{4.5}$$

$$J_l\ddot{\theta}_l + T_{fl}(\dot{\theta}_l) + k_\alpha\alpha = 0\,, \tag{4.6}$$

$$\alpha = \theta_l - \theta_u\,. \tag{4.7}$$

The difference between the angular positions of the lower and upper disc, the torsion angle of the string, is indicated by α. T_{fl} expresses the friction torque acting on the bearings of the lower disc. From [2] and [4], it is learned that the friction torque in the bearings can be modeled with a symmetric friction function

$$T_{fl}(\dot{\theta}_l) = \begin{cases} T_l(\dot{\theta}_l)sign(\dot{\theta}_l) & for \quad \dot{\theta}_l \neq 0 \\ [-T_l(0), T_l(0)] & for \quad \dot{\theta}_l = 0, \end{cases} \tag{4.8}$$

with

$$T_l(\dot{\theta}_l) = Tc_l + b_l\left|\dot{\theta}_l\right|. \tag{4.9}$$

Here Tc_l represents the Coulomb friction and b_l the viscous contribution to the friction torque of the lower part.

4.2.2 Parameter estimation using a simulated measurement

The parameters of the lower part of the set-up are being estimated by the same procedure as is used for estimating the parameters of the upper part in section 4.1.2. In [2], the parameters as given for P_{ref} in table 4.2 were found. These parameters are being used to generate a simulated measurement. The initial parameter set P_0 (see table 4.2) differs slightly from P_{ref}. The following objective function is being minimized

$$\min \sum_{i=1}^{n} \left(\theta_{l,i} - \hat{\theta}_{l,i}\right)^2. \tag{4.10}$$

Only the angular displacement of the lower disc is taken into account in (4.10). The angular displacement of the upper disc θ_u can be minimized in (4.10) too, since it is influenced by the movement of the lower disc, and therefore by the parameters of the lower disc. However, doing so did not produce better parameter estimation results for the parameters of the lower disc. Executing the minimization procedure yields the set of parameters P as given in table 4.2. Applying P to the model, results in a simulated angular displacement of the lower disc $\hat{\theta}_l$ and a torsion angle $\hat{\alpha}$ as depicted in figures 4.3 and 4.4, respectively. In figures 4.5 and 4.6 the results for the validation signal are depicted. In table 4.2 it is visible that P differs more from P_{ref} than P_0 does, while the errors which are depicted in figures 4.3-4.6 are pretty small. Apparently, a parameter set which differs from P_{ref} can produce accurate estimation results. For smaller differences between P_{ref} and P_0, P does resemble P_{ref}.

Table 4.2: Estimated parameter set P, describing the simulated displacement.

	J_l [kg·m^2]	k_α [Nm/rad]	Tc_l [Nm]	b_l [Nms]
P_{ref}	0.0414	0.0775	0.0171	0.0092
P_0	0.0550	0.0900	0.0200	0.0130
P	0.0498	0.0930	0.0202	0.0108

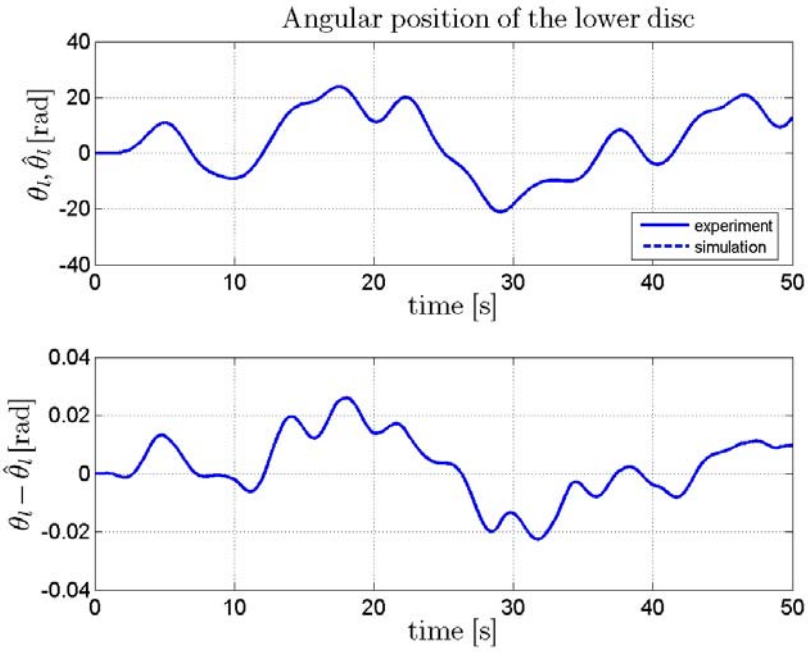

Figure 4.3: Estimation results for θ_l, using a simulated data set; R^2=1.0000.

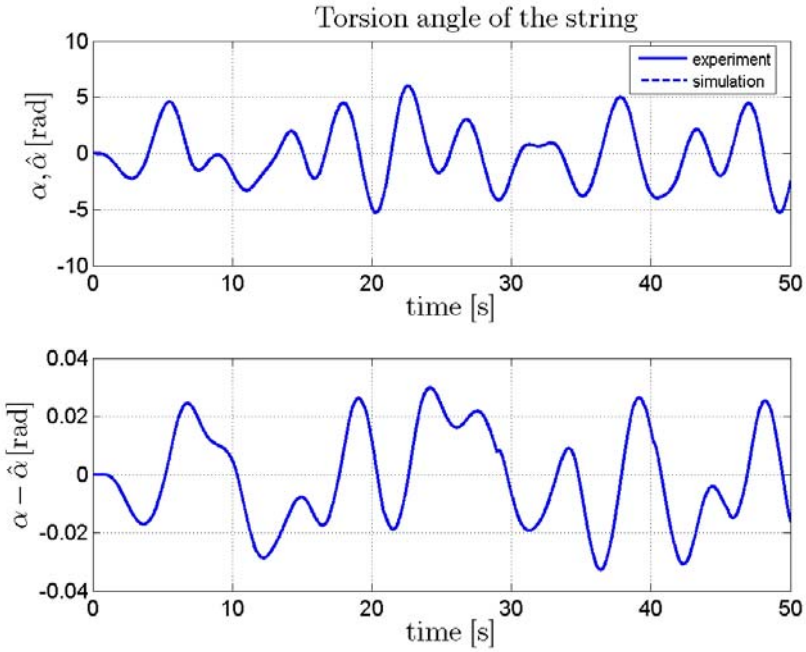

Figure 4.4: Estimation results for α, using a simulated data set; R^2=1.0000.

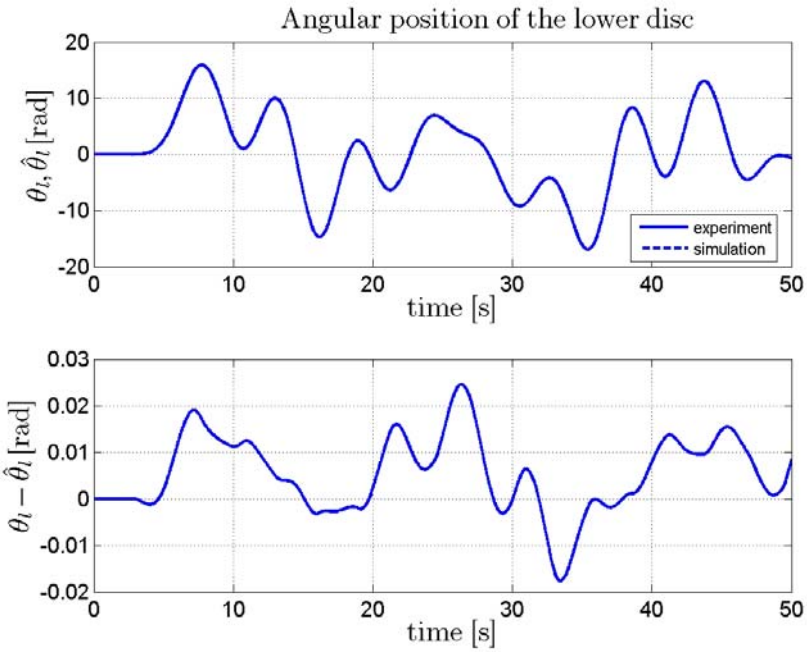

Figure 4.5: Validation results for θ_l, using a simulated data set; R^2=1.0000.

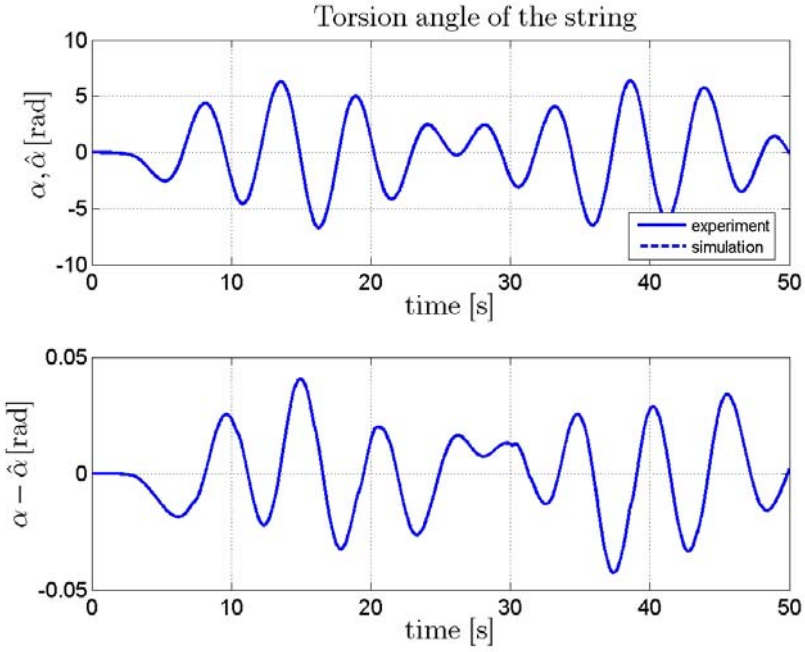

Figure 4.6: Validation results for α, using a simulated data set; R^2=1.0000.

4.3 Lower part of the set-up including brake

4.3.1 Modeling the lower part including brake

The system of the lower part with brake is very similar to the system as described in section 4.2.1. The difference is that a different friction torque acts on the lower part. The dynamics of the complete set-up are expressed by

$$J_u\ddot{\theta}_u + T_{fu}(\dot{\theta}_u) - k_\alpha\alpha = k_m u\,, \tag{4.11}$$

$$J_l\ddot{\theta}_l + T_{flb}(\dot{\theta}_l) + k_\alpha\alpha = 0\,, \tag{4.12}$$

with α as defined in (4.7) and

$$T_{flb}(\dot{\theta}_l) = \begin{cases} T_{lb}(\dot{\theta}_l)sign(\dot{\theta}_l) & for \quad \dot{\theta}_l \neq 0 \\ [-T_{lb}(0), T_{lb}(0)] & for \quad \dot{\theta}_l = 0 \end{cases} \tag{4.13}$$

and

$$T_{lb}(\dot{\theta}_l) = Tc_{lb} + b_{lb}\left|\dot{\theta}_l\right| + (Ts_{lb} - Tc_{lb})e^{-\left(\frac{|\dot{\theta}_l|}{\omega_{sl}}\right)^{\delta_{sl}}}\,. \tag{4.14}$$

Clearly, b_{lb} represents viscous friction and Ts_{lb} equals the static friction, $-T_{lb}(0^-)=T_{lb}(0^+)=Ts_{lb}$. Tc_{lb} represents the Coulomb friction, ω_{sl} represents the Stribeck velocity and δ_{sl} the Stribeck shape parameter.

4.3.2 Parameter estimation using a simulated measurement

The parameter set P_{ref}, found in [2], is used to generate a simulated measurement for the lower part including brake. The values of the initial parameter set P_0 are listed in table 4.3. These values are pretty close to P_{ref}. It has been noticed that when a bigger difference between P_{ref} and P_0 is taken, the parameter estimation procedure will stop prematurely; yielding an estimated parameter set P which does not resemble P_{ref}, but P_0 instead. In that case the estimation accuracy is very low. The objective function which is being minimized equals (4.10). By making use of the set of estimated parameters P, and by applying the estimation and validation signals to the model, figures 4.7- 4.10 are calculated. These figures represent the displacement of the lower disc and the torsion angle for the estimation and validation signal respectively.

Table 4.3: Estimated parameters of the lower part including brake.

	Tc_{lb} [Nm]	b_{lb} [Nms]	Ts_{lb} [Nm]	ω_{sl} [rad/s]	δ [-]
P_{ref}	0.0473	0.0105	0.2781	1.4302	2.0575
P_0	0.0490	0.0120	0.2850	1.6000	2.1500
P	0.0478	0.0109	0.2796	1.4367	2.0731

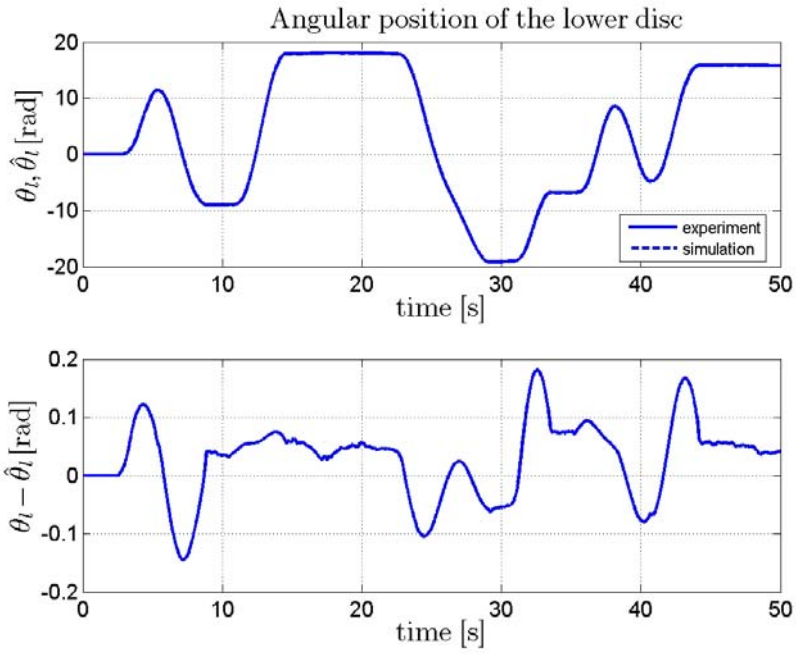

Figure 4.7: Estimation results for θ_l, using a simulated data set; R^2=1.0000.

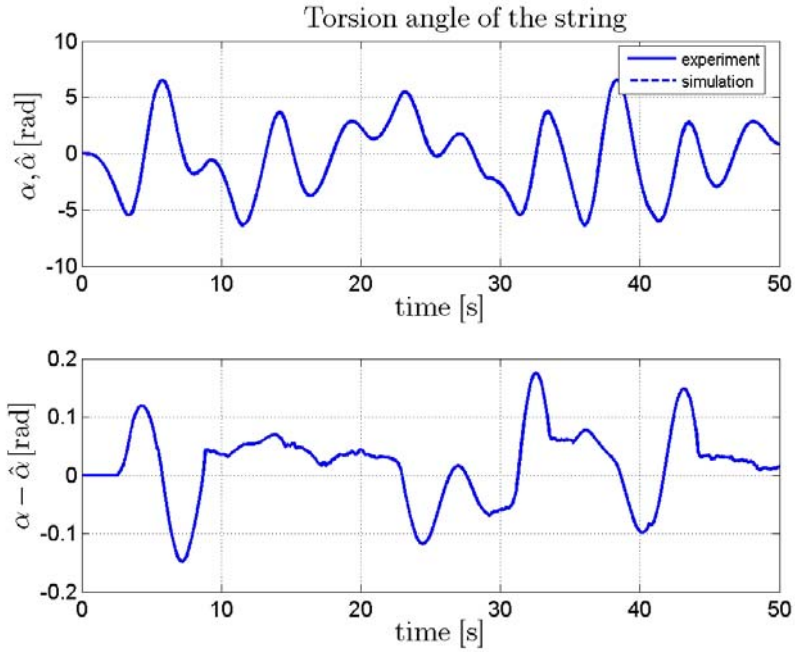

Figure 4.8: Estimation results for α, using a simulated data set; R^2=0.9996.

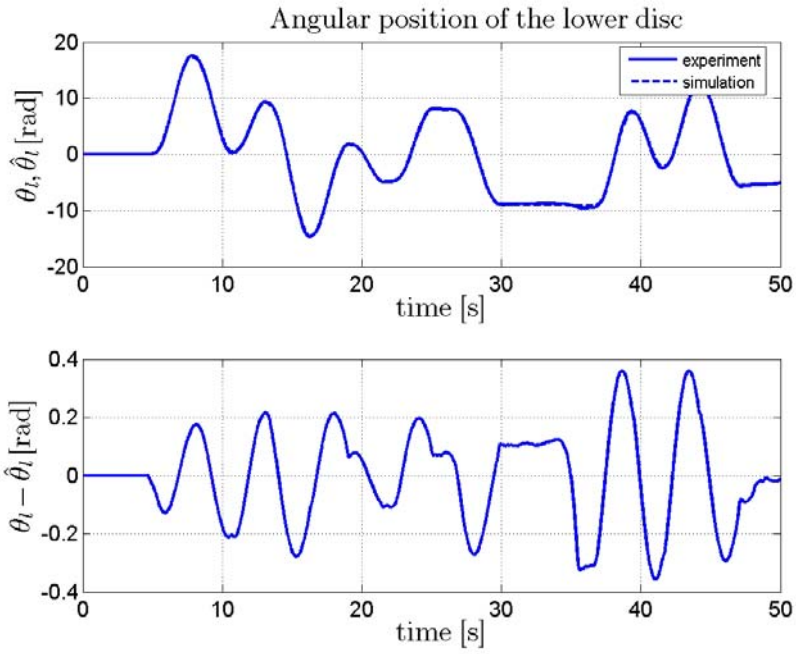

Figure 4.9: Validation results for θ_l, using a simulated data set; R^2=0.9995.

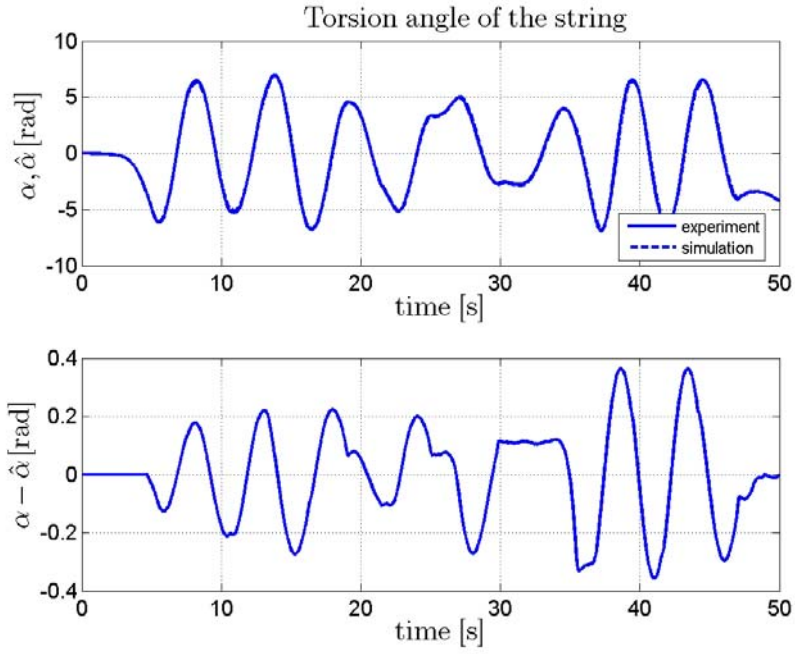

Figure 4.10: Validation results for α, using a simulated data set; R^2=0.9986.

It has been noticed that, especially for the lower part including brake, the initial set of parameters P_0 shouldn't differ too much from P_{ref}, in order to obtain resemblance between the finally estimated parameter set P and P_{ref}. Otherwise, the estimation procedure will encounter local minima, which cause the estimation procedure to stop. However, no resemblance between P and P_{ref}, does not imply that P does not produce accurate estimation results. In general, it can be concluded that the simulated displacement is described pretty accurately even when P does not resemble P_{ref}.

The above implies that the estimation procedure applied to real experimental data, presumably will only give approximate values of the actual parameters. Moreover, the initial set of parameters P_0 has a very big influence on the finally estimated parameter set P. Therefore, the errors between experiment and simulation are studied, followed by adapting P_0. This is an essential step in the parameter estimation procedure, since it may increase the quality of the estimated parameters drastically.

Chapter 5

Parameter estimation using experimental data

In chapter 4, the parameters were estimated using a simulated experiment. The estimation procedure has proven to be accurate when the initial set of parameters was close enough to the actual parameter set. In this chapter, the parameters of real measurements are determined by using the same estimation procedure as is proposed in chapter 3 and used in chapter 4. However, the measurement data are no longer generated by a model, but by applying the input voltages from figure 3.2 to the DC motor of the experimental set-up instead. Subsequently, the displacements θ_u and θ_l of the upper and lower disc are measured.

5.1 Upper part of the set-up

5.1.1 Modeling the upper part

The parameters of the upper part of the set-up are being estimated first. In order to ensure that the friction at the lower part does not influence the dynamics of the upper disc, the string is removed. The equations of motion for the upper part are the same as given in subsection 4.1.1. For clarity they are repeated here

$$J_u\ddot{\theta}_u + T_{fu}(\dot{\theta}_u) = k_m u\,, \tag{5.1}$$

where

$$T_{fu}(\dot{\theta}_u) = \begin{cases} T_u(\dot{\theta}_u)sign(\dot{\theta}_u) & for \quad \dot{\theta}_u \neq 0 \\ [-T_u(0), T_u(0)] & for \quad \dot{\theta}_u = 0, \end{cases} \tag{5.2}$$

with

$$T_u(\dot{\theta}_u) = Tc_u + \Delta Tc_u sign(\dot{\theta}_u) + b_u\left|\dot{\theta}_u\right| + \Delta b_u\dot{\theta}_u\,. \tag{5.3}$$

The Coulomb friction torque for 0^+ rad/s equals $Tc_{up}=Tc_u+\Delta Tc_u$ and for 0^- rad/s $Tc_{un}=Tc_u-\Delta Tc_u$. Viscous friction torque is represented by $b_{up}=(b_u+\Delta b_u)\cdot\omega_u$ for positive and $b_{un}=(b_u-\Delta b_u)\cdot\omega_u$ for negative angular velocities.

The value of the moment of inertia of the upper disc J_u about its center of mass can be calculated easily, using

$$J_u = \rho_u \frac{\pi}{32} D_u{}^4 t_u\,. \tag{5.4}$$

The density ρ_u of steel is $7.9\cdot10^3$ kg/m^3, the diameter D_u = 0.40 m and thickness t_u = 2.4 cm. This results in J_u =0.4765 kg·m^2.

5.1.2 Parameter estimation of experimental data from the upper part

Now, the parameters of the upper part are to be determined using measurement data from [2] and [4]. The following objective function is being minimized:

$$\min \sum_{i=1}^{n} \left(\theta_{u,i} - \hat{\theta}_{u,i} \right)^2 \tag{5.5}$$

The set of initial parameters P_0 (table 5.1) equals the estimated parameter set for the upper part from [2]. It was noticed that the error for positive velocities was higher than it was for negative velocities, while the estimation procedure was terminated since the objective function was smaller than the predefined tolerance. By decreasing the initial parameters which describe friction for positive velocities, and starting the estimation procedure again, parameter set P was obtained (table 5.1). Using P, a simulated angular displacement is obtained. The measured and simulated displacements are depicted in figure 5.1. The error between measured and simulated angular displacement $\theta_u - \hat{\theta}_u$ is depicted at the bottom of figure 5.1. Validation results are shown in figure 5.2. The R^2-criterion for estimation and validation equals 1.0000 and 0.9993, respectively; so the model and corresponding estimated parameter set describe reality very well.

Table 5.1: Estimated parameter set P, describing experimental data.

	k_m [Nm/V]	Tc_u [Nm]	ΔTc_u [Nm]	b_u [Nms]	Δb_u [Nms]
P_0	4.3228	0.3798	-0.0058	2.4245	-0.0084
P	4.3687	0.3827	-0.0076	2.4506	-0.0079

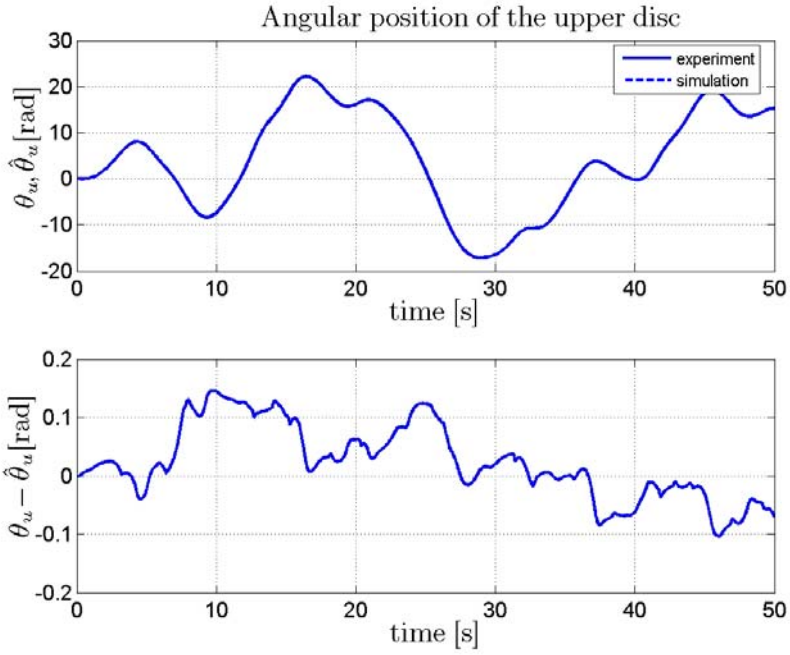

Figure 5.1: Estimation results for θ_u, using a measured data set; R^2=1.0000.

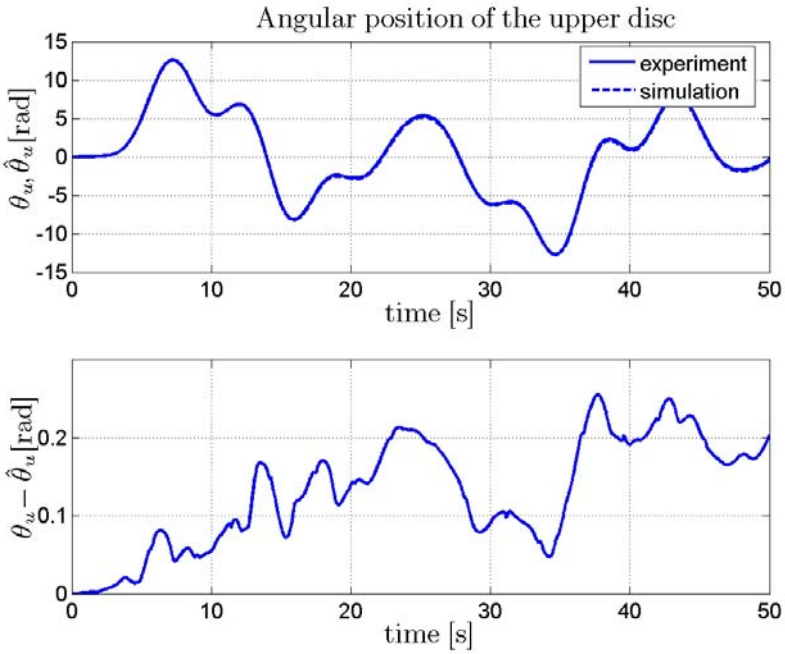

Figure 5.2: Validation results for θ_u, using a measured data set; R^2=0.9993.

From figures 5.1, 5.2 and the R^2-criterion values, which are close to 1, it is concluded the quality of the parameter estimation was very high. Therefore, these estimated parameter values are used for the upper part during the other estimation steps. The friction values read Tc_{up}=0.3752, Tc_{un}=0.3902, b_{up}=2.4427 and b_{un}=2.4585, which means that the friction torque for positive angular velocities is lower. Calculating (5.2) and (5.3) using these friction values, results in an asymmetric friction torque curve as shown in figure 5.3.

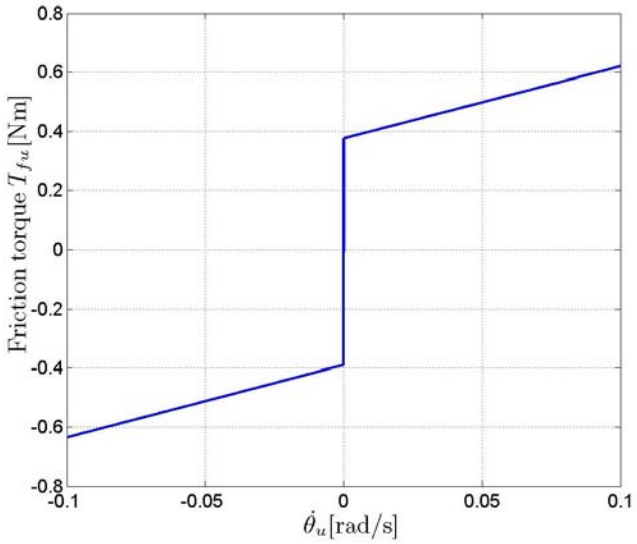

Figure 5.3: Estimated friction torque of the upper part.

5.2 Lower part of the set-up

The parameter identification procedure of the lower part is done according to the method described in chapter 3. In this section, the friction in the lower bearings, the moment of inertia of the lower disc and the stiffness of the string are going to be determined. This means that the brake is not applied and the string is attached to the upper and lower disc.

5.2.1 Modeling the lower part

The equations of motion for the lower part are the same as given in subsection 4.2.1 they are

$$J_u\ddot{\theta}_u + T_{fu}(\dot{\theta}_u) - k_\alpha\alpha = k_m u\,, \tag{5.6}$$

$$J_l\ddot{\theta}_l + T_{fl}(\dot{\theta}_l) + k_\alpha\alpha = 0\,, \tag{5.7}$$

with

$$\alpha = \theta_l - \theta_u\,, \tag{5.8}$$

and

$$T_{fl}(\dot{\theta}_l) = \begin{cases} T_l(\dot{\theta}_l)sign(\dot{\theta}_l) & for \quad \dot{\theta}_l \neq 0 \\ [-T_l(0), T_l(0)] & for \quad \dot{\theta}_l = 0, \end{cases} \tag{5.9}$$

where

$$T_l(\dot{\theta}_l) = Tc_l + b_l\left|\dot{\theta}_l\right|. \tag{5.10}$$

It is clear that no distinction has been made between the friction torque for positive and negative angular velocities.

An initial value for k_α is calculated using

$$k_\alpha = \frac{ED^4\pi}{64(1+\upsilon)L}\,, \tag{5.11}$$

with Young's modulus of steel E=2.0·10^{11} N/m^2, diameter D=2·10^{-3} m, Poisson ratio υ=1/3 and the length of the string L=1.47 m. Calculating (5.11), yields k_α=0.080 Nm/rad. The value of k_α is known from previous estimations too. Since the estimation results from [2] are used for the initial set of parameters P_0, k_α is chosen to equal the estimated value found in [2], k_α=0.0775. Compared to the calculated k_α, the estimated value does not differ very much, so it is plausible that the estimated value represents k_α well indeed.

5.2.2 Parameter estimation of experimental data from the lower part

In [2], the parameter values as given in table 5.2 were found. This set is used to have an initial set P_0 for the estimation procedure. The following objective function is being minimized:

$$\min \sum_{i=1}^{n} \left(\theta_{l,i} - \hat{\theta}_{l,i} \right)^2 \tag{5.12}$$

Applying the estimation procedure to experimental data from [2] and [4], yields the set of parameters P given in table 5.2. Using the parameter set P and the estimation signal for the model, results in an angular displacement of the lower disc as shown in figure 5.4 and a torsion angle as depicted in figure 5.5. The quality of the estimated parameters is high, since R^2_θ=0.9996 and R^2_α=0.9987 for the estimation signal. Next, the validation signal and the same set of parameters P are applied to the model; yielding R^2_θ=0.9991 and R^2_α=0.9981. Validation results are shown in figure 5.6 and 5.7. From these figures, it becomes clear that the errors for the validation signal are higher than they are for the estimation input signal. This is explained by the fact that the parameters were estimated using the estimation signal, so it can be expected that these parameters yield less accurate results for the validation signal. However, adapting P_0 in order to obtain better validation results, did not result in smaller errors for both the estimation and validation signal. Therefore, the parameter set P is proposed to describe the parameters of the lower part.

Table 5.2: Estimated parameter set P, describing experimental data.

	J_l [kg·m^2]	k_α [Nm/rad]	Tc_l [Nm]	b_l [Nms]
P_0	0.0414	0.080	0.0171	0.0092
P	0.0414	0.0775	0.0171	0.0089

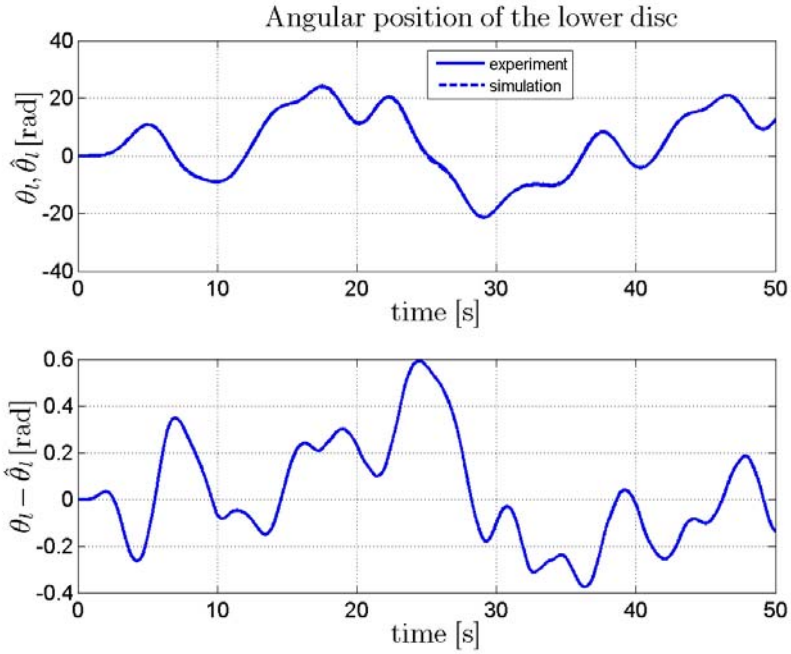

Figure 5.4: Estimation results for θ_l, using a measured data set; R^2=0.9996.

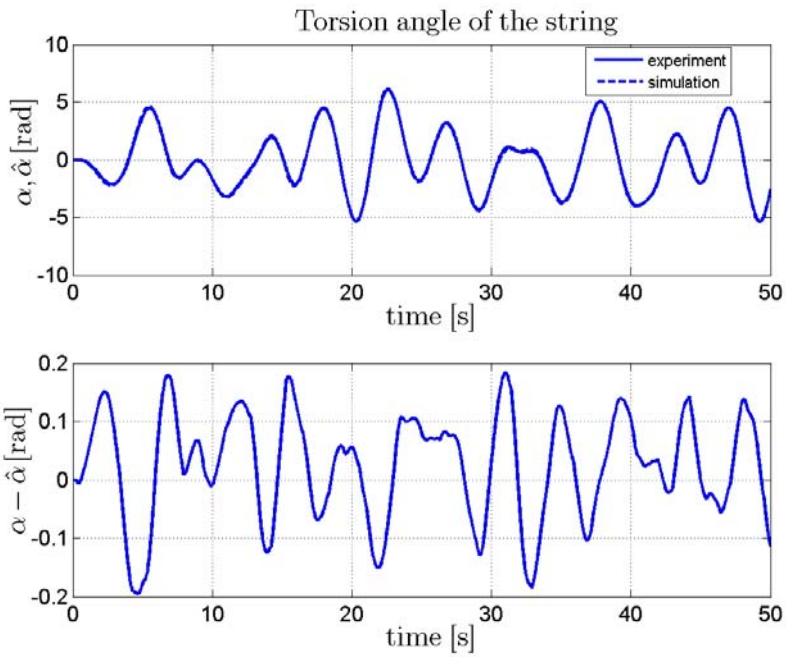

Figure 5.5: Estimation results for α, using a measured data set; R^2=0.9987.

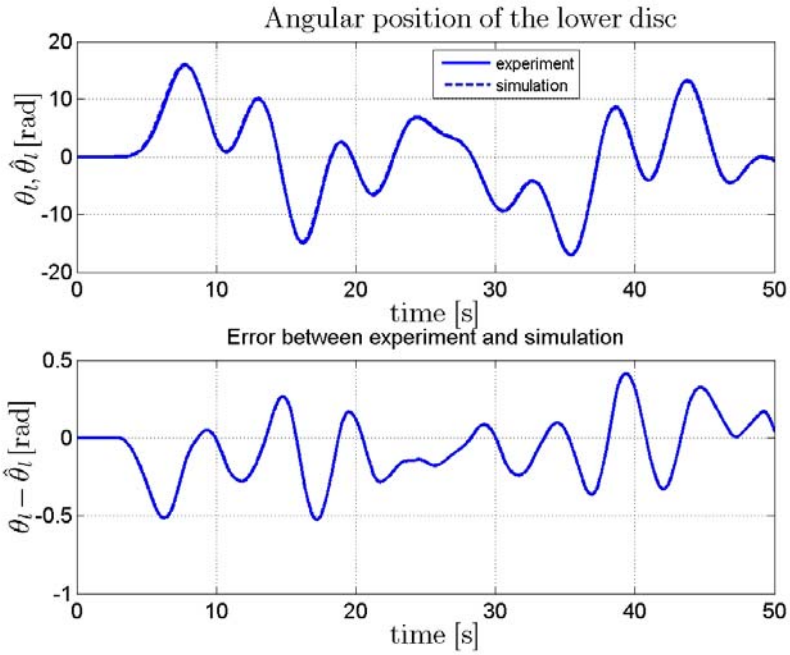

Figure 5.6: Validation results for θ_l, using a measured data set; R^2=0.9991.

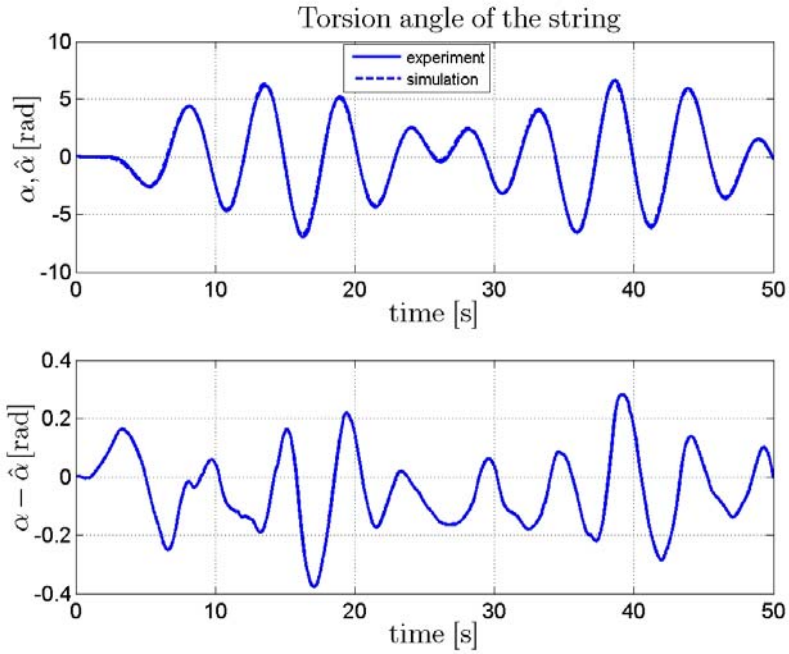

Figure 5.7: Validation results for α, using a measured data set; R^2=0.9981.

5.2.3 Parameter estimation using an asymmetric friction model

The error between measured and simulated angular displacement is pretty large (almost 0.6 radians). To achieve a smaller error, it is decided is to use an asymmetric friction model instead

$$T_{fl}(\dot{\theta}_l) = \begin{cases} T_l(\dot{\theta}_l) sign(\dot{\theta}_l) & for \quad \dot{\theta}_l \neq 0 \\ [-T_l(0), T_l(0)] & for \quad \dot{\theta}_l = 0, \end{cases} \tag{5.13}$$

with

$$T_l(\dot{\theta}_l) = Tc_l + \Delta Tc_l sign(\dot{\theta}_l) + b_l \left|\dot{\theta}_l\right| + \Delta b_l \dot{\theta}_l \,. \tag{5.14}$$

The parameter estimation procedure is started again, using the same experimental data and initial set of parameters P_0 as in section 5.2.2, nevertheless with an asymmetric friction model this time. In table 5.3 the estimated parameters are shown.

Table 5.3: Estimated parameter set P, describing experimental data.

	J_l [kg·m^2]	k_α [Nm/rad]	Tc_{lp} [Nm]	Tc_{ln} [Nm]	b_{lp} [Nms]	b_{ln} [Nms]
P_0	0.0414	0.0775	0.0171	0.0171	0.0089	0.0089
P	0.0414	0.0775	0.0139	0.0244	0.0093	0.0079

It is clear that there is a difference in friction values for positive and negative velocities. More precisely: the Coulomb friction for negative velocities is larger than it is for positive velocities while viscous friction is larger for positive velocities.
Parameter set P is applied to the model. The R^2-criterion for the displacement of the lower disc is the same as for the symmetric friction model ($R^2_{\theta l}$=0.9996) while the maximum error is lower (compare figures 5.4 and 5.8). The R^2-criterion for the torsion angle of the string has slightly improved to 0.9990.

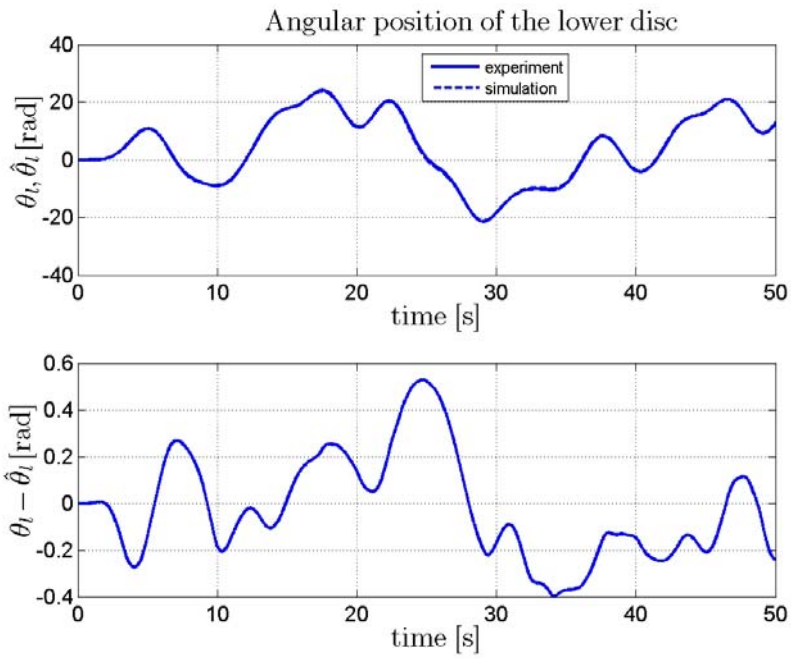

Figure 5.8: Estimation results for θ_l, using the asymmetric friction model; R^2=0.9996.

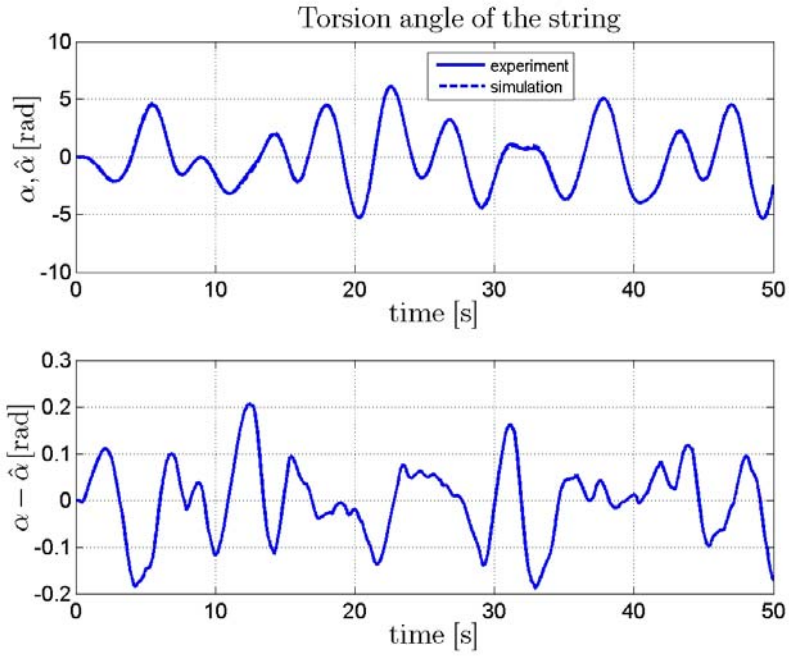

Figure 5.9: Estimation results for α, using the asymmetric friction model; R^2=0.9990.

Since the asymmetric friction model gives slightly better results, this model is chosen. Validation of parameter set *P* from table 5.3 yields the validation results as depicted in figures 5.10 and 5.11.

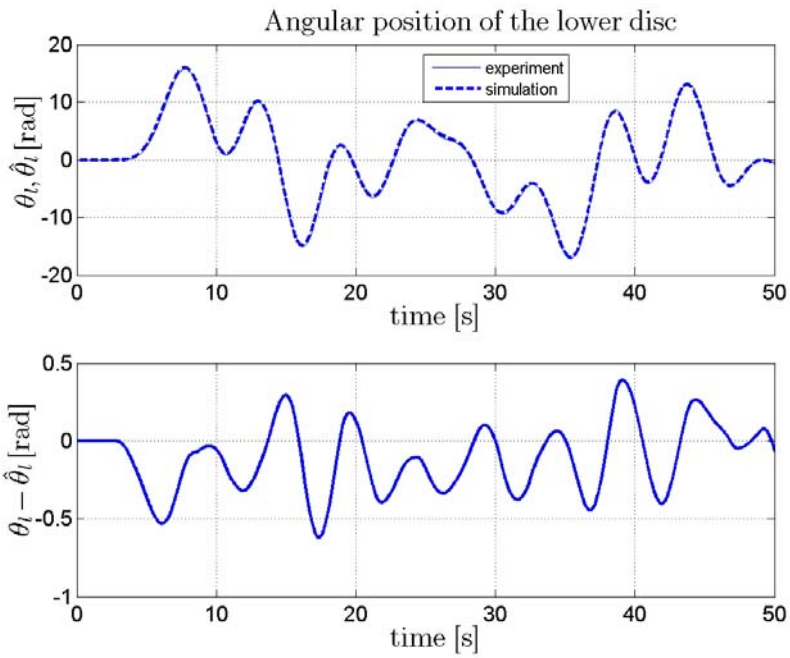

Figure 5.10: Validation results for θ_l, using the asymmetric friction model; R^2=0.9989.

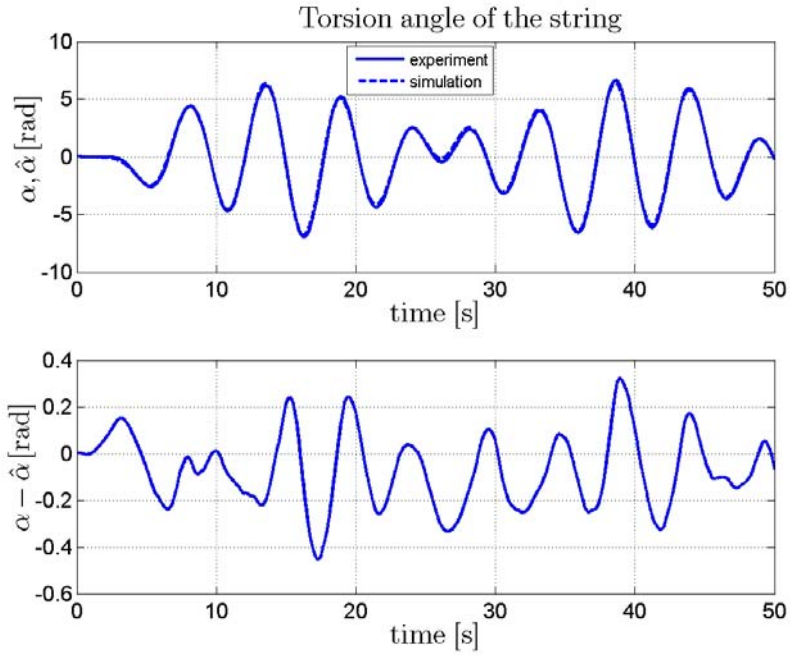

Figure 5.11: Validation results for α, using the asymmetric friction model; R^2=0.9978.

The R^2-criterion values for the validation input voltage are a little bit lower than they were for the symmetric friction model. However, since the maximum errors for the estimation signal are smaller, the asymmetric friction model is chosen to describe friction in the lower bearings. Calculating equations (5.13) - (5.14), using the estimated set of parameters P from table 5.3, results in the friction model in figure 5.12.

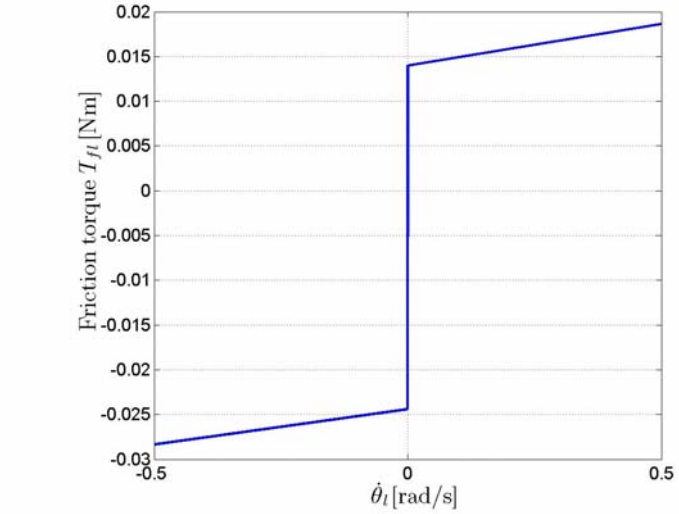

Figure 5.12: Estimated asymmetric friction torque for the lower part.

5.3 Lower part of the set-up including brake

In the previous sections, the following components have been discussed: the upper part, the stiffness of the string, friction at the lower bearings and the moment of inertia of the lower disc. In this section, the parameters which describe the friction function of the brake are going to be determined.

5.3.1 Modeling the lower part including brake

The equations of motion for the lower part including brake are similar to the ones as stated in subsection 4.3.1. However, in the previous section, friction for the lower part has been modeled by an asymmetric friction model. This asymmetric contribution is taken into account for the friction model of the lower part with brake as well.

In real drill string systems negative damping has been observed between the drilling bit and the borehole. In the experimental set-up negative damping is created by lubricating the brake disc with ondina oil. This causes torsional vibrations with stick-slip to occur for a range of constant input voltages, see [2] and [4]. This observation justifies to use a friction model with negative damping contributions as in(5.18).

The equations for the total set-up are described by

$$J_u\ddot{\theta}_u + T_{fu}(\dot{\theta}_u) - k_\alpha\alpha = k_m u\,, \tag{5.15}$$

$$J_l\ddot{\theta}_l + T_{flb}(\dot{\theta}_l) + k_\alpha\alpha = 0\,, \tag{5.16}$$

with

$$T_{flb}(\dot{\theta}_l) = \begin{cases} T_{lb}(\dot{\theta}_l)sign(\dot{\theta}_l) & for \quad \dot{\theta}_l \neq 0 \\ [-T_{lb}(0), T_{lb}(0)] & for \quad \dot{\theta}_l = 0 \end{cases} \tag{5.17}$$

and

$$T_{lb}(\dot{\theta}_l) = Tc_{lb} + b_{lb}\left|\dot{\theta}_l\right| + \Delta b_{lb}\dot{\theta}_l + (Ts_{lb} - Tc_{lb})e^{-\left(\frac{|\dot{\theta}_l|}{\omega_{sl}}\right)^{\delta_{sl}}}\,. \tag{5.18}$$

Here, Δb_{lb} represents the asymmetric viscous contribution to the friction model for the lower part with brake. The viscous friction for positive velocities is expressed by $b_{lbp}=b_{lb}+\Delta b_{lb}$ and $b_{lbn}=b_u-\Delta b_u$ for negative angular velocities. It is assumed that the Coulomb friction can be described with a symmetric friction model for negative and positive angular velocities. This assumption is made since it is learned from [2] and [4], that especially the value of the stick friction of the brake is much higher than it is for the bearings of the lower part. Therefore, the asymmetric contribution of the bearings of the lower part is negligibly small in the stick region. For nonzero angular velocities, the asymmetric Coulomb friction contribution from the lower part is not taken into account either, since the aforementioned assumption is applicable to some extent and to keep the computational complexity of the system low.

5.3.2 Parameter estimation using experimental data

Using the same methodology as in sections 5.1 and 5.2, the parameters in (5.18) are determined from experimental results. However, some problems arise when determining a parameter set from just one experiment. As is depicted in figure 5.13, four experiments yield four different measured displacements for the lower disc, while the input signals for these experiments are exactly the same.

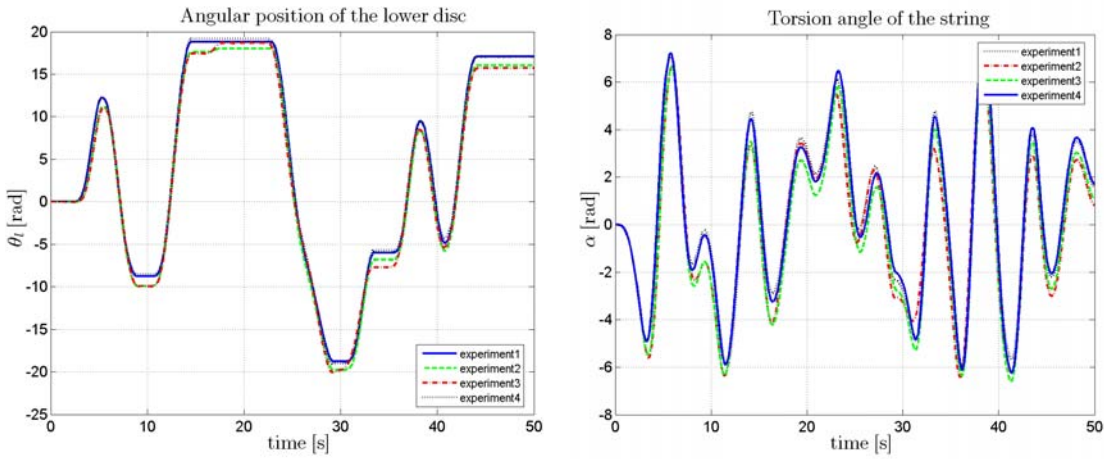

Figure 5.13: Experimental results angular displacement lower disc including brake.

The discrepancy is attributed to the initial difference between the position of the lower and upper disc, resulting in a winded string ($\alpha_0 \neq 0$ at $t=0$). Since the sticktion effect is present in the friction at both the upper and lower part, a prewinded string is very hard to avoid, resulting in a possible initial torsion angle α_0, which varies for each experiment. Therefore the estimation procedure is not executed on a single experiment, but on these four experiments instead. In this way a parameter set P is obtained which will describe an average experiment. P is obtained by minimizing (5.19)

$$\min \sum_{k=1}^{m} \sum_{i=1}^{n} \left(\theta_{l,i,_k} - \hat{\theta}_{l,i} \right)^2 . \tag{5.19}$$

This function minimizes the sum of objective functions for four different experiments, where m indicates the number of experiments. This results in one parameter set which optimally describes the four experiments from figure 5.13. However, the estimated set is a compromise since none of the experiments is described perfectly.

In [2], the parameters as given in table 5.4 were found. This set was the optimal set to describe all experiments with. Here, it is used as the initial guess P_0 for the parameter estimation procedure of four experiments, done in [2] and [4]. Applying the estimation procedure on these four experiments, yields the set of parameters P listed in table 5.4.

Table 5.4: Estimation results from four different experiments.

	Tc_{lb} [Nm]	b_{lbp} [Nms]	b_{lbn} [Nms]	Ts_{lb} [Nm]	ω_{sl} [rad/s]	δ_{sl} [-]
P_0	0.0473	0.0105	0.0105	0.2781	1.4302	2.0575
P	0.0430	0.0096	0.0089	0.2832	1.4502	1.7504

The R^2-criterion values for these experiments are listed in table 5.5, they give a measure for the resemblance of the estimated and the measured data.

Table 5.5: Estimation quality for four experiments.

	Experiment 1	Experiment 2	Experiment 3	Experiment 4
$R^2_{\theta l}$	0.9957	0.9945	0.9973	0.9992
R^2_{α}	0.9716	0.9651	0.9685	0.9905

In figures 5.14 and 5.15 the simulated displacement of the lower disc and the torsion angle are depicted, together with the four experiments from which P is determined. It is visible that the estimated displacement seems to be an “averaged” experiment of the four different experimental displacements. Using the criterion (5.19), this observation was to be expected. The R^2-criterion is highest for experiment four. Therefore, the angular displacement of the lower disc ($\theta_{4,l}$) and torsion angle (α_4) from experiment four are chosen to depict the error between the experimental and simulated displacement.

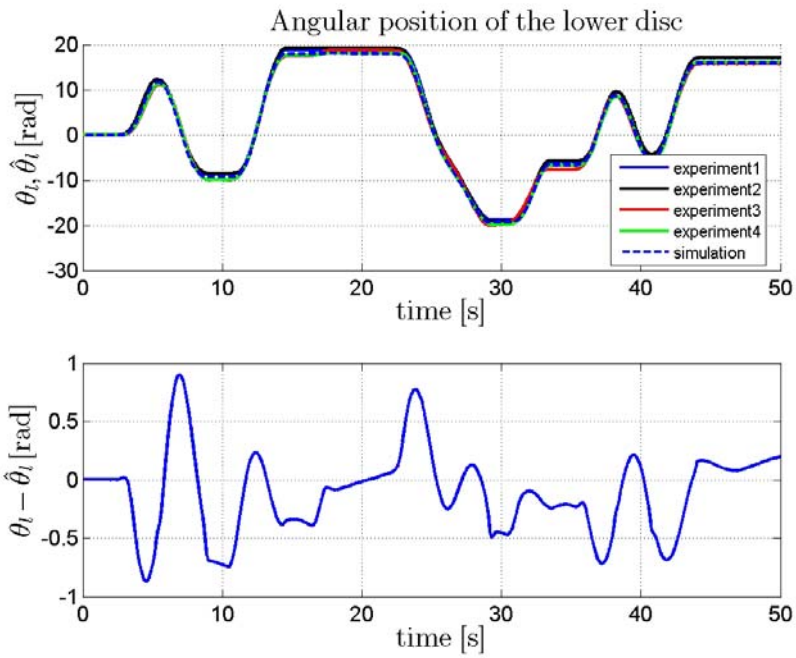

Figure 5.14: Estimation results using an experimental data set, R^2=0.9992.

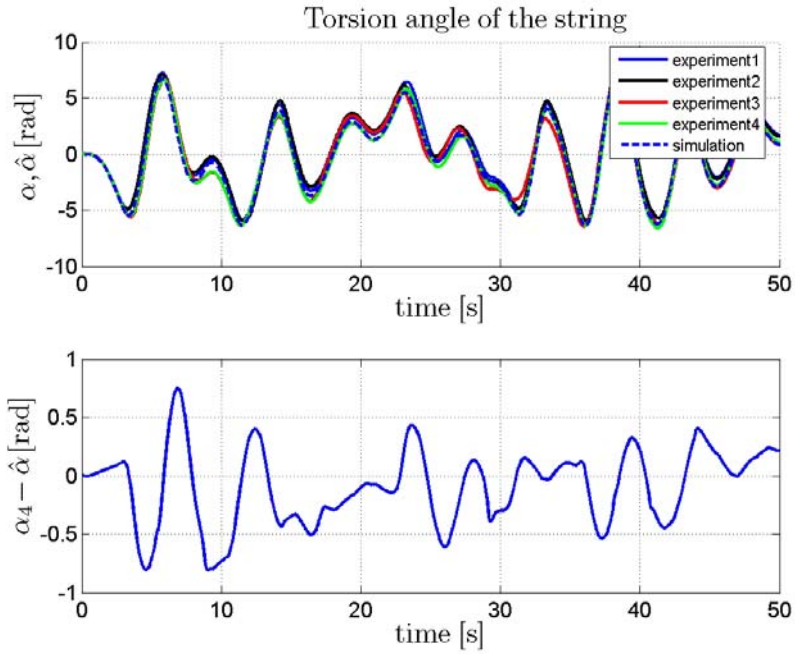

Figure 5.15: Estimation results using an experimental data set, R^2=0.9992.

The simulated results for the estimation signal are satisfying, so the validation results for P as given in table 5.4 are depicted below as well, with $R^2_{\theta l}$=0.9869 and R^2_{α}= 0.9757.

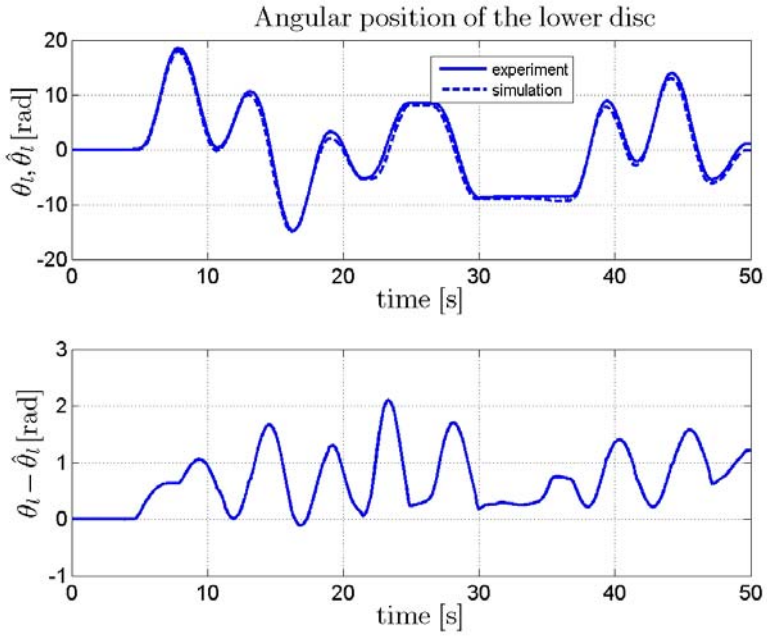

Figure 5.16: Validation result lower part with brake, R^2_{θ}=0.9869.

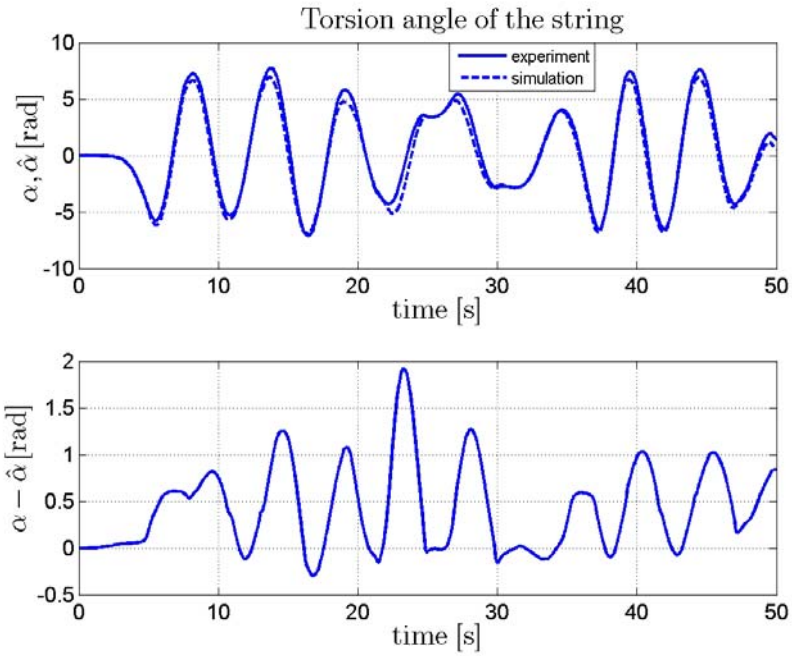

Figure 5.17: Validation result lower part with brake, R^2_{α}=0.9757.

The previously displayed results indicate high parameter estimation quality. The error between simulated and experimental data is small and the R^2-values for both estimation and validation are close to 1. From figure 5.16, it can be derived that the error between experiment and simulation reaches its maximum value when the angular velocity of the lower disc does as well. Also, the error is mainly positive for the validation results, which means that the simulated displacement is smaller than the measured, experimental displacement. For the estimation signal, the error is small and it is more evenly distributed for positive and negative angular velocities.

These observations indicate that it is very plausible that the estimated parameter set describes reality well. Therefore this set of parameters is chosen. Using (5.17) and (5.18), the friction torque curve as shown in figure 5.18(a) is calculated. Negative damping is clearly present up to approximately 3 rad/s, caused by a fluid film between brake blocks and brake disc. From 3 rad/s, linear viscous friction dominates, causing the friction model to be linear for relatively high angular velocities. In figure 5.18(b), zoomed in is on the friction torque for very low angular velocities. It is visible that positive damping is present up to 0.016 rad/s, and then the negative damping region starts.

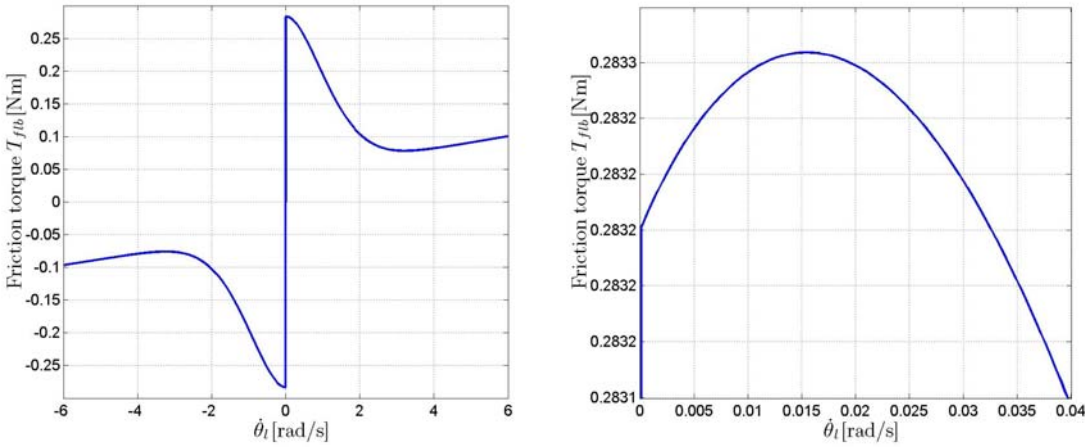

(a) (b)

Figure 5.18: Friction torque for the lower part including brake.

Chapter 6

Conclusions and recommendations

In this thesis, a rotor dynamic system, which exhibits the same type of stick-slip vibration phenomena as found in drilling systems, has been examined. This system mainly consists of two rotating discs which are attached to each other by a low stiffness string. Due to friction forces which are caused by the bearings of the lower disc and a brake on top of it, the lower disc stalls repetitively for a range of input voltages (i.e. stick-slip vibrations exist). To describe the dynamical behavior of the experimental set-up, the equations of motion are formulated. The parameters in these equations have been estimated in this work based on experimental data.

6.1 Conclusions

The experimental set-up is driven by a DC motor which is controlled by an input voltage. By estimating the parameters of the equations of motion of the set-up bit by bit, the effect of the input voltage on the movement of the set-up has been described accurately. First, the parameter estimation for the upper part of the set-up has been carried out. The estimated parameters gave very accurate results as confirmed by validation experiments. Then, the stiffness of the string and the parameters of the lower part were determined without applying the brake. The estimated set of parameters gave satisfying results as well. Finally, the parameters of friction for the brake were determined. Here, the error between simulation and experiment was larger. This is mainly caused by different initial conditions for each experiment, resulting in a less accurately estimated set of parameters. In general the estimation results were very good.

Although the error between measurement and simulation was very small in general, an error always occurred. This could have been caused by numerous reasons. Most importantly, a model will never describe reality exactly. Especially for low angular velocities the error between experiment and simulation got larger. This may be caused by a friction torque which is more complex for very low angular velocities than was stated in the model. Also the influence of the initial set of parameters on the error for the estimation procedure is very high. Several trials may be needed to reach optimal results. Finally, the experiment itself may be disturbed in some non-reproducible way. The estimated parameters, however, in general describe the set-up accurately.

6.2 Recommendations

- An important cause for non-reproducible results is that the drill string was winded over an unknown angle at the start of the experiment. This can be prevented by using a device to line out the upper and lower disc more accurately before starting the experiment.

- Research can be done on friction models which describe low angular velocities better.

- Another measure to indicate the resemblance between experiment and simulation should be searched for. The R^2-criterion gives a somewhat distorted indication, since the error for values lower than 0.95 is very large, while one would not suspect so from a value which is very close to one. For example, a measure that indicates the relative difference between experiment and simulation, may give a better indication about the magnitude of the error.

Bibliography

[1] T.R. Fenner. *Mechanics of solids*. Blackwell Scientific Publications, 1989.

[2] M.P.M. Hendriks. *Analysis of torsional and lateral vibrations in an experimental drill string set-up.* Master's thesis, Eindhoven University of Technology, 2004.

[3] J.L. Meriam, L.G. Kraige. *Engineering Mechanics Dynamics*. John Wiley &Sons, 2000.

[4] N. Mihajlović. *Torsional and Lateral Vibrations in Flexible Rotor Systems with Friction.* PhD thesis, Eindhoven University of Technology, 2005.

[5] A.A. van Veggel. *Modelling of drill-string set-up and experimental evaluation of friction induced limit cycling.* Master's thesis, Eindhoven University of Technology, 2002.